TECHNICAL MEMORANDUM

X-717

OPTIMIZATION OF NUCLEAR-ROCKET POWERPLANT PARAMETERS

By Paul G. Johnson, Glenn R. Cowgill,
and James W. Miser

Lewis Research Center
Cleveland, Ohio

RESTRICTED DATA

1954

CLASSIFIED DOCUMENT - TITLE UNCLASSIFIED

This material contains information affecting the national defense of the United States within the meaning of the espionage laws, Title 18, U.S.C., Secs. 793 and 794, the transmission or revelation of which in any manner to an unauthorized person is prohibited by law.

NATIONAL AERONAUTICS AND SPACE ADMINISTRATION

WASHINGTON

February 1963

E-1479

This document released to Category C-91, Nuclear Reactors for Rocket Propulsion. (M-3679 (27th Ed.), November 15, 1962.

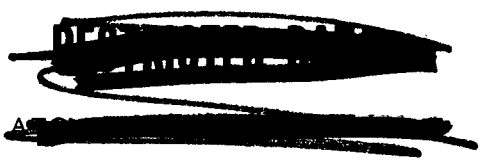

NATIONAL AERONAUTICS AND SPACE ADMINISTRATION

TECHNICAL MEMORANDUM X-717

OPTIMIZATION OF NUCLEAR-ROCKET POWERPLANT PARAMETERS*

By Paul G. Johnson, Glenn R. Cowgill, and James W. Miser

SUMMARY

A method of nuclear-rocket powerplant optimization is presented and illustrated with an example corresponding to the initial phase of a man-manned Mars exploration mission. The analysis is intended to determine the values of reactor flow area, reactor-exit pressure, and reactor length that produce maximum residual load. (Residual load is defined as the payload plus all items not included in the powerplant, vehicle structure, propellant, and tankage.) Assumptions and equations are presented in detail. The example analysis shows that, for the application of an advanced nuclear-rocket powerplant to a 1,000,000-pound Mars vehicle, the attainment of high specific impulse has a strong effect on the choice of powerplant parameters. Optimum pressure is shown to be relatively low and optimum reactor dimensions are relatively large, which resulted in low reactor-power density and high powerplant specific weight. Furthermore, the optimization is insensitive to changes in powerplant parameters, so that large off-optimum deviations result in residual load reductions of only a few percent.

INTRODUCTION

The selection of design-point values of powerplant parameters for any type of propulsion system involves a complex interplay of mission, vehicle, and powerplant characteristics. The optimum compromise among all the operative factors is seldom, if ever, attained. Early studies that indicate the important trends and approximately optimum values, however, are vital to the success of a system development program. The analysis is usually straightforward in principle but complex because of

*Title, Unclassified.

the many system components and their mutual interdependence. The analyst's greatest problem is the prediction of component performance and weight at a date prior to hardware testing.

Nuclear rockets may be advantageously applied to several types of mission. The optimum combination of powerplant parameters will be different for each application. Nuclear-rocket powerplants for spacecraft that start from a low-altitude orbit about the Earth are studied herein. Similar analyses could be undertaken for surface-launch or suborbital upper-stage applications of nuclear rockets.

The principal components of the nuclear-rocket system are propellant and tank, reactor assembly, nozzle, propellant feed system, nuclear shield, and vehicle structure. The sum of all other components, such as payload, vehicle controls, and navigation equipment, is termed residual load.

The reactor assumed for this study is moderated and reflected by water, which is circulated through the core and the reflector where it is cooled by a water-hydrogen heat exchanger. The reactor assembly includes the core, reflector, pressure shell, reactor control system, heat exchanger, and water pump and lines. The hydrogen propellant flows from the tank through the booster pump, main pump, nozzle walls, reflector, water heat exchanger, reactor core, and nozzle. A small portion of the hot hydrogen is bled from the exit of the reactor, mixed with cold hydrogen leaving the nozzle wall, and then exhausted through the turbine which drives the hydrogen and water pumps.

The principal parameters that may be varied by the powerplant designer are reactor flow area, reactor-exit pressure, and reactor length. These parameters are subject to optimization, which is complicated by the intricate coupling of the various powerplant components and by the requirement that payload be the measure of merit. Certain other quantities have physical limits determined by materials, properties, or geometry. Examples of such limits are maximum fuel-element temperature, maximum reactor-exit dynamic pressure or Mach number, and minimum fuel-element hydraulic diameter. Use of the limiting values of these quantities will usually result in the highest attainable vehicle performance. The values of thrust, specific impulse, and powerplant weight calculated for each combination of parameters are used to determine vehicle performance for each specified mission and stage weight. Optimum values of flow area, pressure, and reactor length can then be determined on the basis of maximum residual load.

This report presents the optimization method and shows typical results for one powerplant type. Previous attempts to optimize powerplant parameters for orbital-launch nuclear rockets have been of a more preliminary nature (refs. 1 and 2). Component studies, such as those made

in conjunction with the overall vehicle investigation summarized in reference 3, have provided data for a more comprehensive solution of the problem herein.

ANALYSIS

Method

The basic method of powerplant optimization is a straightforward calculation of vehicle performance for each combination of independent variables and optimization parameters. Optimization is achieved through a comparison of values of residual load, which is defined as the payload plus all items not included in the powerplant, vehicle structure, propellant, and tankage. Two aspects of the method, which will be given special consideration herein, are (1) the assumed characteristics of the several powerplant and vehicle components, and (2) the method of multiparameter optimization.

Each powerplant type may require individualized treatment because the physical limits of one may differ from those of another that is of contrasting composition or design. For example, the reactor core analyzed herein is characterized by the use of thin, metallic fuel elements. Dynamic loadings of such fuel elements are expected to establish the maximum feasible gas flow per unit area at a specified pressure level. For a more rigid fuel-element configuration, the limit might be gas velocity, pressure drop, or thermal stress. The analysis described in the following section uses the dynamic pressure ($\rho V^2/2g \equiv \gamma p M^2/2$) as a physical limit. (Symbols are defined in the appendix.)

Two other quantities are fixed at their estimated limiting values on the assumption that maximum vehicle performance will result therefrom. Maximum fuel-element temperature is set by the properties of the materials, the fabrication techniques, and the required operating life. Minimum fuel-element spacing is determined by structural arrangement and allowable tolerances. In the absence of experimental tests or design studies of fuel-element configurations, limiting values have been assumed for both of these parameters and were based on general considerations of physical properties and applicable design practice. In a more detailed study of a particular reactor design, the interrelation of fuel-element temperature, fuel-element spacing, reactor-exit dynamic pressure, and various practical design considerations should be evaluated.

The parameters that may be optimized are (1) reactor flow area, (2) reactor-exit hydrogen pressure, and (3) reactor length. These variables are of direct significance to the powerplant designer, whereas such commonly quoted parameters as thrust, reactor power, and specific impulse are derived quantities. The optimization will be

affected by nuclear-stage gross weight and the velocity requirements of the mission. For the analysis reported herein, however, only one value of gross weight and one mission velocity requirement are investigated.

Powerplant Component Characteristics

The nuclear-rocket model for the analysis is shown schematically in figure 1. The reactor concept is characterized by the use of water as the moderator. Liquid hydrogen flows from the low-pressure tank to a turbopump, which consists of a booster pump, a main pump, and a bleed-driven turbine. The high-pressure propellant from the pump cools the nozzle and the liquid moderator (by means of a water-to-hydrogen heat exchanger in the reflector region) before making its final-heating pass through the reactor core and being expelled through the nozzle. In a water-moderated reactor the moderator makes the circuit shown by the dashed lines. Cold water (1) enters the core from the water pump, (2) makes two core passes during which it is heated internally by nuclear radiations and externally by forced convection removal of reject heat from the fuel-element regions, (3) transfers the heat to the hydrogen in the heat exchanger, and (4) returns to the pump. The hydrogen bleed flow to drive the turbine is visualized as a mixture of hot and cold propellant gases mixed in a manifold near the reactor exit. Turbine exhaust is available for vehicle attitude control. Reactor controls and powerplant controls are also included in the weight of the powerplant. The components are described more fully in the following sections.

Reactor. - The reactor characteristics that directly influence the optimization of powerplant parameters are:

(1) Reactor-exit hydrogen temperature T_e as a function of maximum fuel-element temperature $T_{fe,max}$ and a flow-geometry parameter $(G_R d_{fe})^{0.2}/(L_R/d_{fe})$, which is, in turn, a function of P_e, T_e, L_R, q_e, and d_{fe}

(2) Reactor-passage pressure ratio P_i/P_e as a function of reactor-exit Mach number M_e and the flow-geometry parameter $(G_R d_{fe})^{0.2}/(L_R/d_{fe})$

(3) Reactor weight W_R and diameter D_R as functions of reactor void area A_v and reactor length L_R

Exit temperature and pressure ratio are determined from a heat-transfer and pressure-drop analysis that accounts for multipassage effects, thermal radiation between fuel elements, dissociation and other property changes in the hydrogen, and axial and radial power distributions. The computation procedure is described in reference 4 along with

a correlation of typical results. Reactor weights and diameters are evaluated by criticality calculations similar to those described in reference 5.

The reactor type selected for optimization is a water-moderated, tungsten-fuel-element concept. The tungsten is assumed to be enriched in the isotope tungsten 184 (W^{184}). The criticality calculations are based on the following assumptions:

Homogeneous bare core composition,	water, tungsten, uranium dioxide
Effective multiplication factor, k_{eff}	1.05
Volume ratio of UO_2 to $(UO_2 + W)$	0.15
Weight of tungsten per unit void volume, $W_W/A_V L_R$, lb/cu ft	400
Enrichment of tungsten with tungsten 184, percent	78
Enrichment of uranium with uranium 235, percent	93

Tungsten weight per unit void volume is specified instead of per unit void cross-sectional area (ref. 5) because d_{fe} rather than L_R/d_{fe} is fixed. The further assumption is made that homogeneous bare core weights and diameters adequately approximate the results of more complex analyses of heterogeneous side-reflected reactors. Reactor flow area is obtained from void area by assuming that A_V/A_{ff} is 1.425.

Reactor diameter and weight are presented as functions of void cross-sectional area and reactor length in figure 2. Changes in length are shown to have only a small effect on diameter. The diameter values are in basic agreement with the core dimensions of the HTRE-1, a similar water-moderated reactor described in reference 6.

For preliminary optimization purposes, account need be taken of only the overall weight and diameter characteristics, flow passage configuration, estimated power distributions, and limiting values of dynamic pressure and maximum fuel-element temperature. The tungsten fuel elements are assumed to be flat plates stacked in multiple arrays. The power generation in the fuel plates is assumed uniform except for the outer plates, each of which generates 10 percent more power than any one of the inner plates. The axial power distribution is a cosine curve that goes to zero at either end of the reactor core, and the radial distribution is uniform from one fuel-element assembly to another. Limiting values of fuel-plate spacing s_{fe}, reactor-exit dynamic pressure q_e, and maximum fuel-element temperature $T_{fe,max}$ are assumed to be 0.06 inch, 20 pounds per square inch absolute, and 5460° R, respectively.

Reactor-inlet temperature has only a small influence on overall core heat-transfer and pressure-drop characteristics. Consequently,

for the reactor heat-transfer calculation, a simple approximation is used:

$$T_i = T_{N,i} + \Delta T_{N,ref} \frac{\theta^*}{\theta^*_{ref}} + \frac{Q_X}{Q_R} \frac{\bar{c}_{p,R}}{\bar{c}_{p,X}} (T_e - \Delta T_N - T_{N,i}) \qquad (1)$$

where $T_{N,i}$ is the nozzle-coolant inlet temperature (50° R), and the second and third terms specify the hydrogen temperature rise across the nozzle and heat exchanger, respectively; $\Delta T_{N,ref}$ is the nozzle coolant temperature rise for a reference calculation (from ref. 3) at a temperature difference θ^*_{ref} between hot gas and coolant at the nozzle throat, and Q_X/Q_R is the fraction of total reactor power that is transferred from the moderator to the propellant in the heat exchanger (0.06535). Nozzle coolant temperature at the throat is assumed to equal $T_{N,i} + 0.5\ \Delta T_N$, and $\Delta T_{N,ref}/\theta^*_{ref}$ is evaluated to equal 0.017 from a calculation reported in reference 3. All hydrogen physical properties are obtained from references 7 and 8.

The correlations of reactor-exit temperature and core-pressure drop that result from use of the calculation procedure of reference 4 are shown in figure 3. In figure 3(a), the difference between $T_{fe,max}$ and T_e is plotted as a function of a flow-geometry parameter $(G_R d_{fe})^{0.2}/(L_R/d_{fe})$ and the maximum fuel-element temperature $T_{fe,max}$. Pressure does not enter this correlation. Also in figure 3(b), a pressure-drop parameter $\Delta p_R/p_e M_e^2$ is plotted as a function of the same flow-geometry parameter and reactor-exit Mach number M_e. The pressure-drop curves are so nearly independent of $T_{fe,max}$ that this variable has been ignored. The curves in figure 3 are not sensitive to anticipated deviations in inlet temperature, plate emissivity, or power distribution between plates.

Pressure shell. - The reactor is enclosed in a pressure shell consisting of a cylindrical section and a dome-shaped head. The thickness of the cylindrical shell is determined by hoop stress

$$b_{PS} = \frac{D_R P_{X,i}}{2\sigma_{PS}} \qquad (2)$$

The dome head is assumed to weigh 50 percent more than a disk of diameter D_R and thickness b_{PS}. The weight of the basic cylinder and

dome is increased by 20 percent to account for fittings and other structural features. Thus,

$$W_{PS} = 0.6\ \pi \frac{D_R^2 L_R P_{X,i}}{\left(\frac{\sigma}{\rho}\right)_{PS}} \left(1 + 0.375\ \frac{D_R}{L_R}\right) \tag{3}$$

A value of $(\sigma/\rho)_{PS}$ of 32,400 pounds per square foot per pound per cubic foot is used, based on titanium properties at moderator temperature. Maximum design stress is about 50 percent of ultimate tensile stress.

Reactor control system. - The weight of the reactor control system, which consists of rods or drums, actuators, and associated sensing and decision-making equipment, is assumed to be proportional to reactor volume above a minimum weight of 100 pounds; that is,

$$W_{RC} = 20\left(\frac{\pi}{4} D_R^2 L_R\right) \tag{4a}$$

or

$$W_{RC} = 100 \text{ lb} \tag{4b}$$

whichever is greater. The constant of proportionality is evaluated by assuming that the control rods occupy 2 percent of the reactor volume and have an average density of 500 pounds per cubic foot. The control rods are assumed to account for one-half the reactor control system weight.

Moderator cooling and circulation components. - Two special powerplant components must be considered when the reactor moderator is a liquid. A pump is provided to circulate the moderator out of the core, and a heat exchanger is provided to cool the moderator. In the water-moderated reactor concept, the water is assumed to be cooled by the hydrogen leaving the nozzle cooling passages. The water pump is to be driven by a hot-gas-bleed turbine, which may be separate or the same unit that drives the hydrogen turbopump if satisfactory control and speed matching can be achieved.

The weight of the water pump and associated piping is assumed to be proportional to the water-flow rate. The constant of proportionality is

evaluated on the basis of typical, advanced-design liquid pumps and estimated pipe lengths:

$$W_{WP} = 0.5\ w_m \tag{5}$$

For low-flow systems a minimum weight is established at 40 pounds.

The heat exchanger could be optimized by means of parametric studies of different heat-transfer-surface configurations. Such a complete treatment is beyond the scope of a powerplant optimization study and not likely to improve the overall results significantly over what can be achieved with a simplified approach. Consequently, the assumptions are made that the water-to-hydrogen heat exchanger is of the counterflow tube-and-shell type (with hydrogen inside the tubes) and has the following fine geometry:

Tube inside diameter, in.	0.1435
Tube outside diameter, in.	0.1875
Tube arrangement	Equilateral triangle
Tube centerline spacing, in.	0.225

Hydrogen total temperatures and pressures at exchanger inlet and exit are assumed equal to the corresponding values at nozzle cooling-passage exit and reactor inlet, respectively. The number of tubes is determined by assigning a value of 0.2 to the exit hydrogen Mach number $M_{X,e}$ in the equation

$$N_t = \frac{w}{\left(\frac{\pi}{4}\right) D_{in}^2\ p_{X,e}\ M_{X,e}} \sqrt{\frac{Rt_{X,e}}{g\gamma_{X,e}}} \tag{6}$$

Because the heat-exchanger and reactor structure is aluminum, maximum moderator temperature is fixed at 660° R. Minimum water temperature is varied so as to yield a minimum tube temperature of 550° R. These two temperature limitations prevent ice formation in the heat exchanger and ensure core structure temperatures compatible with aluminum.

The local convective heat-transfer coefficient on either surface is computed by using the film-temperature correlation with appropriate substitutions:

$$Nu_f = 0.021\ Re_f^{0.8}\ Pr_f^{0.4} \tag{7}$$

where the subscript f means that the hydrogen properties (including density) are evaluated at the film temperature

$$t_f = 0.5(t_b + t_w) \tag{8}$$

The pressure change in either fluid is calculated by means of the relation

$$\Delta p = \frac{G^2}{g}\left(\frac{1}{\rho_1} - \frac{1}{\rho_2}\right) - 4f\,\frac{\Delta L}{d}\,\frac{G^2}{2g\bar{\rho}} \tag{9}$$

where G is the mass velocity; d is the hydraulic diameter; ρ_1, ρ_2, and $\bar{\rho}$ are the initial, final, and average densities, respectively, (evaluated at film temperature) in the length interval ΔL; and the friction factor f is evaluated by the turbulent-flow equation

$$f = \frac{0.046}{Re_f^{0.2}} \tag{10}$$

Tube length L_t is determined by step-by-step calculations of temperature and pressure along the tube length and an iterative procedure to satisfy all the prescribed temperature and flow-rate conditions. Water-flow rate is determined when the value of minimum moderator temperature is reached that satisfies the no-icing requirement. The total heat rate is specified to be 7 percent of reactor core power (6.535 percent of total reactor power). Nuclear radiation heating of the water in the heat exchanger is neglected.

Heat-exchanger weight is the sum of tube and water weights increased by 20 percent to account for shell, headers, and other structural items:

$$W_X = 1.2\left[\pi\rho_t L_t N_t\left(D_{out} - \frac{D_{out} - D_{in}}{2}\right)\left(\frac{D_{out} - D_{in}}{2}\right) + \rho_m\left(\frac{\sqrt{3}}{2}\,s_t^2 - \frac{\pi}{4}\,D_{out}^2\right)\right] \tag{11}$$

where tube density ρ_t is assumed to be 174 pounds per cubic foot and water density varies with temperature.

Nozzle. - A complete analysis of a regeneratively cooled exhaust nozzle would include (1) contour determination, (2) length optimization,

(3) cooling-passage design with consideration of thermal radiation and other local conditions, and (4) investigation of multichannel and pressure-drop effects, which limit the coolant velocity. Nozzle weight and attainable specific impulse would influence the length optimization. Such a complex treatment is beyond the scope of this powerplant optimization.

A less rigorous approach is adopted herein. The assumption is made that a comparison of the local heat flux and the rate of pressure drop at the nozzle throat can be used to relate any nozzle to a reference design. Thus the normalized temperature and pressure variations along the nozzle length are fixed for the entire family of nozzles in accordance with the results of a more extensive design study (ref. 3). Maximum nozzle wall temperatures will be limited by the properties of the materials used. Although a thin-wall nozzle of tubular construction would involve the least extension of the chemical-rocket state of the art, preliminary calculations indicate that such a nozzle could not be regeneratively cooled for the gas temperatures assumed herein. A throat-wall temperature far exceeding the limits of steels or nickel-base alloys would be encountered. Consequently, an insulated-wall construction is postulated, in which molybdenum is used for the gas-side surface. Gas-side throat-wall temperature $T^*_{w,g}$ is fixed at 3500° R and coolant-side throat-wall temperature $T^*_{w,c}$ is fixed at 1860° R. The required ratio of wall thermal conductivity to wall thickness k_w/b_w is variable but within the range achievable with a thin region of stagnant hydrogen.

Different correlations of heat-transfer coefficient are employed on the two sides of the nozzle wall. The equation used for gas-side convection is

$$Nu_f = 0.027\ Re_f^{0.8}\ Pr_f^{0.33} \tag{12}$$

where the subscript f means that the hydrogen properties (including density) are evaluated at film temperature

$$t^*_{g,f} = 0.5(t^*_g + T^*_{w,g}) \tag{13}$$

On the coolant side the correlation used for anticipated throat pressures and temperatures (ref. 9) is that used in the heat exchanger:

$$Nu_f = 0.021\ Re_f^{0.8}\ Pr_f^{0.4} \tag{7}$$

where the film temperature is

$$t^*_{c,f} = 0.5(t^*_c + T^*_{w,c}) \tag{14}$$

The ratio of wall thermal conductivity to wall thickness is a function of heat flux; therefore,

$$\frac{k_w}{b_w} = \frac{q^*_g}{T^*_{w,g} - T^*_{w,c}} \tag{15}$$

The throat heat flux is computed from the gas-side heat-transfer coefficient h^*_g evaluated in equation (12):

$$q^*_g = h^*_g(T^*_{aw} - T^*_{w,g}) \tag{16}$$

where the adiabatic wall temperature

$$T^*_{aw} = t^*_g + 0.9(T^*_g - t^*_g) \tag{17}$$

Also, T^*_g is assumed to equal the reactor-exit total temperature T_e, and thermal radiation from the reactor is considered negligible at the throat.

In order to evaluate h^*_c (eq. (7)), assumptions must be made regarding coolant-side total temperature T^*_c and total pressure P^*_c at the nozzle throat. In accordance with the nozzles designed in some detail for reference 3, the assumptions are that

$$T^*_c = T_{N,i} + 0.5\ \Delta T_N \tag{18}$$

and

$$P^*_c = 1.15\ P_{N,e} \tag{19}$$

Another simplification introduced at this point is the assumption that nozzle-cooling computations are not sensitive to the small differences in hydrogen-weight-flow rate caused by extraction of turbine bleed between the coolant and gas-side passes. Thus, identical weight-flow rates are used in equations (12) and (7).

Coolant velocity is a function of flow area as well as flow rate and density. Flow area and passage hydraulic diameter are determined by assuming the nozzle to be composed of square channels. The throat diameter D^* is solved for in the equation:

$$\frac{\pi}{4} D^{*2} = \frac{w}{p_g^* \sqrt{\frac{\gamma_g^* g}{R_g^* t_g^*}}} \tag{20}$$

where γ_g^* and R_g^* are evaluated at t_g^* and p_g^*. When blockage due to channel walls is neglected, the coolant-side hydraulic diameter at the throat is

$$d_c^* = \frac{w}{\pi D^* G_c^*} \tag{21}$$

where G_c^* is the coolant mass velocity at the throat. The corresponding coolant velocity (or Mach number M_c^*) is that value that will satisfy the heat flux balance

$$q_g^* = q_c^* \frac{S_c}{S_g} = h_c^* (T_{w,c}^* - T_c^*) \frac{S_c}{S_g} \tag{22}$$

The channel walls are assumed to act as fins, thereby causing S_c/S_g to exceed unity. The fin effectiveness is computed from

$$\eta_F = \frac{\tanh\left(d_c^* \sqrt{\frac{2h_c^*}{k_F b_F}}\right)}{d_c^* \sqrt{\frac{2h_c^*}{k_F b_F}}} \tag{23}$$

where the assumed value of $k_F b_F$ is 2.22×10^{-6} Btu per second per $^\circ$F.

Thus,

$$\frac{S_c}{S_g} = 1 + 2\eta_F \tag{24}$$

Simultaneous solution of the mass velocity equation

$$G_c^* = p_c^* M_c^* \sqrt{\frac{\gamma_c^* g}{R_c^* t_c^*}} \tag{25}$$

and of equations (7) and (21) to (24) is required. The assumptions are such that M_c^* does not exceed 0.4 for the cases illustrated in this report. The corresponding axial pressure gradient on the coolant side is computed from the equation

$$\frac{1}{P_c^*}\left(\frac{dP_c}{dx}\right)^* = -\frac{\gamma_c^*}{2} M_c^{*2}\left[\frac{1}{T_c^*}\left(\frac{dT_c}{dx}\right)^* + 4\frac{f}{d_c^*}\right] \tag{26}$$

where the friction factor f is assumed to be 0.004 and the axial temperature gradient

$$\left(\frac{dT_c}{dx}\right)^* = \frac{\pi D^* q_g^*}{w c_{p,c}^*} \tag{27}$$

After completion of the throat calculations, overall nozzle temperature rise and pressure drop may be estimated by means of comparisons to the reference nozzle. The temperature rise ΔT_N is assumed to be proportional to the total heat-transfer rate:

$$\Delta T_N = \frac{q_g^* D^{*2}}{w\left(\frac{q_g^* D^{*2}}{\Delta T_N w}\right)_{ref}} \tag{28}$$

where nozzle surface area is proportional to the square of throat diameter. From reference 3, $\left(q_g^* D^{*2}/\Delta T_N w\right)_{ref}$ is evaluated at 0.214 Btu per pound per $^{\circ}F$. The pressure-drop approximation is also based on calculations reported in reference 3:

$$\Delta P_N = \left(\frac{dP_c}{dx}\right)^* \tag{29}$$

[redacted]

where ΔP_N is in pounds per square inch when $(dP_c/dx)^*$ is in pounds per square inch per foot.

Nozzle weight is estimated by relating the computed or measured weights of similar nozzles to a simplified analytical model. No explicit accounting is made for the variation in k_w/b_w. The convergent section is treated as a 45°-half-angle, right-circular cone with its base diameter equal to $0.9\ D_R$ and its thickness determined by hoop stress at the maximum diameter:

$$b_{N,C} = \frac{P_e(0.9\ D_R)}{2\sigma_{N,C}} \tag{30}$$

The weight is increased 40 percent over that of the cone to account for the channel construction and other structural necessities. A ratio of stress to density $(\sigma/\rho)_{N,C}$ for the nozzle structural material of 13,600 ((lb/sq ft)/(lb/cu ft)) is used (Inconel X).

The divergent-section weight is based on a typical contour. An equation with empirically evaluated coefficients has been derived as a result of unpublished NASA design and fabrication experience. The result is included as the second term of the overall nozzle-weight equation:

$$W_N = 4.2\times10^{-5}\ D_R^3 P_e + 6900\ \frac{w}{P_e^{0.667}} \tag{31}$$

where P_e is in pounds per square foot. The first term is the convergent-section weight and incorporates the assumptions described previously. Although the derivation is merely approximate, the equation satisfactorily evaluates the nozzle weight reported in reference 3 and other similar designs. The equation is based on a nozzle with an area ratio of 50.

Specific impulse I_{vac} is evaluated from reactor-exit temperature and pressure in accordance with reference 7, with the assumptions of an area ratio of 50, expansion to vacuum, a velocity correction factor of 0.96, and equilibrium conditions in the expanding gas. The specific impulse data are reproduced in a convenient form in figure 4.

Propellant feed system. - The propellant feed system is assumed to be composed of (1) a turbopump with hot-bleed-driven turbine, (2) a start system, and (3) all related structure and piping. The bleed cycle is chosen because it appears to be "a serious contender for the job" and may be analyzed in a straightforward manner. Details of the handling of

the bleed flow are not analyzed, but the turbine-inlet temperature is specified to be 1860° R; and, in the calculation of piping weight, the assumption is made that the bleed flow originates near the reactor aft face. Turbine exhaust is assumed to be used for roll control and, possibly, vector control. No thrust contribution is attributed to the turbine exhaust.

The liquid hydrogen enters the turbopump from the tank in an essentially boiling condition. A combination of reactor-tank separation distance, shield thickness, and tank pressure is assumed such that the net positive suction head (NPSH) is zero. A boost pump with inducer and vapor separator serves to pump the boiling liquid to a NPSH of 650 feet (20 lb/sq in.) at the main pump inlet. The boost pump design is based on the assumption that the local cooling that accompanies cavitation produces an effective NPSH in the inducer of 50 feet. This effect is called the thermodynamic suppression head (TSH). The main pump raises the propellant to its maximum pressure, the value of which is subject to optimization.

The bleed flow is considered to be a mixture of hot gas from the reactor exit and cold gas from nozzle-cooling-passage exit. The individual weight flows are balanced to give a mixture temperature of 1860° R. The total bleed flow rate is assumed to be proportional to pump flow rate and discharge pressure:

$$w_\beta = \frac{w_{TP} P_{TP,e}}{6,200,000} \tag{32}$$

This equation is based on a turbine pressure ratio of 10 and on turbine and pump efficiencies of 80 percent. These selections are essentially arbitrary in that no specific turbopumps were designed for this study.

The predominant influence of the propellant feed system on the overall propulsion system is its weight. The turbopump is the heaviest component of the feed system. Its weight is approximated by the sum of three terms, representing boost pump, main pump plus turbine, and gears, respectively:

$$W_{TP} = 6 \frac{w_{TP}^{1.16} \Delta P_{BP}}{(NPSH + TSH)^{1.5}} + \frac{10,000 w_{TP} \left(\frac{P_{TP,e}}{500} + 1.1 \right)}{(NPSH + 32.6 \Delta P_{BP})^{1.5}} + 6 w_{TP}^{0.4} \tag{33}$$

All pressures are in pounds per square inch absolute, and NPSH and TSH are in feet. The coefficient and the exponent of w_{TP} in the first

term are based on the boost pump designs reported in appendix C of reference 3. The form of the variation with respect to boost pump pressure rise ΔP_{BP} and effective NPSH is consistent with reference 10. The second term, which gives the sum of main pump and turbine weights, is similar in form to the boost pump relation except that (1) the correlation from reference 3 does not indicate an exponent of w_{TP} greater than unity, and (2) the combined weight is best approximated by two terms, one porportional to $w_{TP}P_{TP,e}$ and the other to w_{TP}. The relative magnitude of the two parts is not indicative of the breakdown between pump and turbine. The third term is a correlation of gear weights from reference 3. If the assumed values of ΔP_{BP}, NPSH, and TSH are used, turbopump weight becomes

$$W_{TP} = 0.34\, w_{TP}^{1.16} + 0.6\, w_{TP}\left(\frac{P_{TP,e}}{500} + 1.1\right) + 6w_{TP}^{0.4} \qquad (34)$$

Turbopump casing and structure weight is included in W_{TP}. In making use of this equation, its empirical nature must be borne in mind. Estimates of turbopump weight seem to vary by factors of two or three from one study to another, and only the development of flight-weight hardware will establish a definitive weight equation. Furthermore, the magnitude of the thermal suppression head must be experimentally established.

The piping and start-system weights are represented by the two terms in the equation

$$W_{SP} = 0.001\, w_{TP}P_{TP,e} + 0.12\, w_{TP} \qquad (35)$$

where $P_{TP,e}$ is in pounds per square inch absolute. The propellant piping is assumed to be made of titanium with the thickness determined by hoop stress. Nominal lengths and velocities are assigned. Similarly, the start system weight is approximate since it is largely a weight of monopropellant.

Powerplant control system. - The flow controls, which coordinate propellant flow rate with reactor power and maintain the desired pressures and temperatures, consist primarily of valves, valve actuators, a flowmeter, temperature sensors, and electronic controls. The assumption is made that the weight of the powerplant control system can be represented by the equation

$$W_{PC} = 0.11\, w_{TP}P_{TP,e}^{0.25} + 30 \qquad (36)$$

where $P_{TP,e}$ is in pounds per square inch absolute. The fixed weight is a nominal value for a minimum system weight.

Vehicle Component Characteristics

In addition to the powerplant and the residual load, the nuclear stage consists of propellant, tanks, nuclear shield, and vehicle structure. The propellant weight is the dominant quantity and is related to powerplant characteristics through the specific impulse and the thrust-to-weight ratio. Tank and structure weights are generally expressed as functions of propellant or stage weight.

Propellant requirements. - The hydrogen propellant weight for a specified mission and a specified initial weight in orbit is a function of effective specific impulse I_{eff} and initial thrust-to-weight ratio F/W_G. Effective specific impulse is less than that of the nozzle flow I_{vac} because of the bleed flow, which is regarded as a loss as far as thrust is concerned. In order to compute the effective specific impulse, the following equation is used:

$$I_{eff} = I_{vac} \frac{W_N}{W_{TP}} \tag{37}$$

During powered flight, thrust is assumed to be constant, continuous, and directed tangent to the velocity vector. Specific impulse is also assumed constant.

Computation of propellant consumption during powered flight is accomplished by numerical integration of the equations of motion. The particular forms of the equations used in the analysis are as presented in reference 11. A Runge-Kutta numerical integration procedure is used to obtain solutions. The Earth is represented by an inverse-square central force field. The radius of the Earth is taken to be 3959 miles and its force constant is assumed to be 95,640 miles^3 per second^2.

Tank. - A simplified approach to the estimation of tank weight is used in the optimization study. The tank weight is assumed to be proportional to the weight of propellant in the tank:

$$W_T = 0.08\ W_{P,T} \tag{38}$$

This weight includes insulation and thermal-radiation shields. The constant of proportionality is adopted from reference 12. The compromise among tank pressure, turbopump weight, reactor-tank separation distance,

and shield weight is not attempted in the analysis reported herein. In addition to adding a large complication to the calculation procedure, such an analysis requires knowledge of propellant mixing while being heated in the tank. This is an area of some disagreement and requires research in zero gravity with internal heat generation.

An allowance for venting and pressurization gas (boiloff hydrogen) is provided by specifying that the propellant in the the tank is percent greater than the amount fed to the powerplant; as a result,

$$W_{P,T} = 1.025\ W_P \tag{39}$$

where W_P is the propellant weight computed in the trajectory analysis.

Nuclear shield. - Without computing the optimum compromise among shield weight, separation distance, tank pressure, and turbopump weight, the shield weight is a rather arbitrary quantity. Its relation to reactor diameter is easily visualized, but its magnitude is more difficult to establish. The base point used for the study is 150 pounds for a 400-megawatt reactor, which is 3.3 feet in diameter (ref. 3). This shield weight represents the amount required to limit propellant heating. Biological shielding and specific mission demands would necessitate additional shielding considerations that are beyond the scope of the powerplant optimization described herein. Thus,

$$W_{NS} = 14\ D_R^2 \tag{40}$$

Use of this equation implies that all propellant tanks subtend the same solid angle from the radiation source and that the effect of observed differences in reactor power is unimportant to the optimization.

Vehicle structure. - The structure that connects the payload, tank, and powerplant is not subjected to high loads during nuclear-powered flight. All appreciable loads, both axial and transverse, are encountered during boost. The nuclear-stage structure is not stressed for boost loads, but the interstage structure between the nuclear vehicle and the booster is assumed to carry these loads during boost and then to be jettisoned. Since launch operations have not been considered in this study, neither interstage weights nor numbers of launch vehicles have been estimated.

The nuclear vehicle structure, which supports the payload and the powerplant from the pressure-stabilized tank, is relatively lightweight. On the basis of references 3 and 12 and other similar studies, the

assumption that vehicle structure weighs 4 percent of the nuclear-stage weight appears reasonable, especially for small stages:

$$W_{ST} = 0.04\ W_G \tag{41}$$

Optimization

The objective of the analysis is to maximize the residual load W_{RL} for the specified combination of gross weight, mission, and limit variables ($T_{fe,max}$, q_e, and s_{fe}). The values of the optimization variables (P_e, A_{ff}, and L_R) corresponding to maximum residual load are referred to as optimum values of these parameters. The parameters are of more importance than the computed magnitudes of residual load; in many cases, the sensitivity of the optimization to changes in these parameters is more significant than the exact optimum values. Therefore, a graphical presentation of the results is of sufficient accuracy and provides a ready visualization of the important trends.

For preliminary calculations, wherein the number of combinations of parameter values is relatively small, a straightforward optimization procedure is acceptable. A value of residual load is calculated for each set of parameter values; the equations and techniques specified herein are used. The results are combined on a plot of W_{RL} as a function of one of the optimization parameters (e.g., P_e) with curves for each combination of the other two parameters (A_{ff} and L_R). An envelope curve can then be drawn enclosing all the curves. The highest point on the envelope curve is the optimum point. Optimum values of the parameters can be read directly or can be estimated from the points of tangency between the envelope curve and the families of curves lying within.

A more complete study of this type might involve too many combinations of parameter values for economical application of the straightforward method. Techniques are available in the field of modern mathematics, such as the method of steepest ascent, which can handle complex multiparameter optimization problems.

RESULTS AND DISCUSSION

Scope of Analysis

The results reported herein were obtained by using the following parameter ranges or values:

Dynamic pressure, q_e, lb/sq in.	20
Maximum fuel-element temperature, $T_{fe,max}$, ^{o}R	5460

[redacted]

Fuel-element spacing, s_{fe}, in.	0.06
Nuclear-stage gross weight, W_G, lb	1,000,000
Mission hyperbolic velocity, V_h, miles/sec	3.5
Reactor flow area, A_{ff}, sq ft	2-7
Reactor-exit pressure, P_e, lb/sq in. abs	200-1000
Reactor length, L_R, ft	3-4

The last three quantities, the optimization parameters, are varied over large ranges in an attempt to include the optimum points and to show any sensitivity of residual load to off-optimum conditions. The listed fuel-element temperature and spacing are representative of anticipated practical limits. The temperature of 5460° R is approximately 80 percent of the melting temperature of tungsten and, therefore, a reasonable operating limit. The spacing of 0.06 inch is believed to be acceptable if care is taken to maintain small tolerances on fuel-element dimensions and minimize relative movement. The nuclear-stage gross weight in orbit is representative of manned interplanetary spacecraft (ref. 12), and the velocity requirement (V_h = 3.5 miles/sec) corresponds to the first propulsion phase of a fast round trip (e.g., a 420-day Mars round trip at the 1980 opportunity). The equivalent velocity increment, from orbital start, is about 2.85 miles per second.

Presentation of Results

The mode of optimization and the presentation of results are illustrated in figures 5 and 6. In figure 5 residual load is plotted as a function of reactor flow area with several curves corresponding to specified values of reactor-exit pressure. The entire family of curves in figure 5 is for specified values of dynamic pressure (20 lb/sq in.), maximum fuel-element temperature (5460° R), fuel-element spacing (0.06 in.), nuclear-stage gross weight (1,000,000 lb), and hyperbolic velocity (3.5 miles/sec). Figures 5(a), (b), and (c) are for reactor lengths of 3, 3.5, and 4 feet, respectively. The dashed line represents an envelope curve, the upper bound of each constant-length family of curves. Each envelope is the locus of maximum-residual-load points over the chosen range of flow area, and the highest point on the envelope is the true optimum point for the specified combination of L_R, q_e, $T_{fe,max}$, s_{fe}, W_G, and V_h. The envelope curves from figures 5(a) to (c) are combined in figure 5(d) to indicate the overall optimum.

Figure 6 presents the same data as in figure 5 plotted in different form. In figure 6 residual load is plotted against reactor-exit pressure with lines of constant reactor flow area. Figures 6(a) to (c) present the results for the three reactor lengths selected, and figure 6(d) summarizes the resulting envelope curves (i.e., the dashed

[redacted]

lines in figures 6(a) to (c)). The significance of the shapes and relative positions of the various curves will be discussed later in the report.

It should be noted that the envelope curves plotted as a function of A_{ff} and P_e are related only at the maximum residual load point. Values of W_{RL} less than the maximum values can be attained by an infinite number of parametric combinations. Thus, envelope curves such as those in figure 5(d) show the maximum residual load, which may be obtained with a specified reactor flow area. In figure 6(d) the maximum attainable values of W_{RL} for specified pressures are shown, but the flow areas required are not illustrated for off-optimum conditions. Thus the envelope curves are presented only to reveal the sensitivity of overall performance to changes in the optimization parameters, and complete data representations such as figures 5 and 6 must be consulted for more detailed information.

In figures 7 and 8, the values of residual load are plotted against reactor-exit temperature and initial thrust-weight ratio, respectively. Since T_e is independent of A_{ff}, the points plotted in figure 7 are the maximum values of W_{RL} for each specified reactor-exit pressure, as read from figure 6. Figure 8 is presented in three parts, one for each value of L_R, and estimated envelope curves are drawn in near the maximum W_{RL} points.

The results of the optimization, presented in figures 5 to 8, show the integrated effect of many factors. A study of this type is chiefly useful to reveal major trends and relations. Consequently, detailed description of the vehicles and powerplants is not attempted. Rather, the results are discussed qualitatively. Because of the many assumptions involved, quantitative results should not be given great attention. For example, the values of residual load shown in the figures are suitable only for relative comparison; a design study would be required to evaluate the payloads reliably. Furthermore, all the results presented herein are for specific conditions (mission, stage weight, materials limits, and component characteristics). Thus the quantitative results have only limited applicability, whereas the qualitative observations may be of more general significance.

Among the more important results of the study are (1) the general magnitudes of the parameter values, which are shown to be near optimum, and (2) the shapes of the various envelope curves. An understanding of the compromises involved in the evaluation of optimum conditions can aid in planning research programs. Similarly, the shapes of the curves reveal the degree of sensitivity of overall performance to changes in the individual parameters. On this basis, early research effort can be concentrated in the most fruitful areas.

Optimization of Flow Area, Pressure, and Reactor Length

The data presented in figures 5 to 7 reveal that the attainment of high specific impulse is a strong factor in the optimization of A_{ff}, P_e, and L_R. Effective specific impulse is a function of reactor-exit pressure and temperature and of bleed-flow rate. The qualitative discussion that follows reviews the principal influences of each parameter in order to arrive at an understanding of the integrated effect.

A reduction in reactor-exit pressure influences I_{eff} in three ways: by (1) reducing the mass velocity G_R and, thereby, increasing reactor-exit temperature T_e (fig. 3(a)); (2) increasing the dissociation-recombination effects, which raises I_{vac} at a specified temperature (fig. 4); and (3) reducing the bleed-flow requirement (eq. (32)). The resulting change in T_e affects I_{vac} to about the same extent as does the dissociation-recombination phenomenon. Since bleed flow is assumed to contribute no thrust, the bleed requirement has a significant effect on I_{eff}, and amounts to as much as the first two influences combined at the higher pressures considered. These three influences tend to lower the optimum pressure.

A reduction in P_e must be accompanied by an increase in reactor flow area in order to maintain the thrust-weight ratio near optimum and prevent excessive gravity loss. The resulting rise in powerplant weight tends to counterbalance the forces acting to reduce P_e. In this respect, the increases in reactor and pressure-shell weights are greater than the reductions in propellant-feed-system weight. Thus, an optimum combination of P_e and A_{ff} will correspond to the point of balance between changes in propellant weight and powerplant weight.

An increase in reactor length influences the overall optimization in two ways: by increasing T_e (fig. 3(a)) and by increasing reactor weight (fig. 2(b)). Coincident effects on pressure drops and other powerplant components weights are secondary. Since the reactor length enters the heat-transfer correlation to the first power in the flow-geometry factor (fig. 3(a)), L_R has a strong effect on T_e and, thus, on I_{vac}. The effect diminishes, however, as T_e approaches $T_{fe,max}$ and as fuel-element-passage length-diameter ratio becomes large. As illustrated in figure 7, equal increments in L_R produce rapidly diminishing increments in T_e.

The net result of these opposing trends is shown in figures 5 and 6. Optimum A_{ff} (fig. 5(d)) is relatively large: about 6 square feet. Optimum P_e (fig. 6(d)) is relatively low: about 400 pounds

per square inch absolute. Optimum L_R is just over 4 feet, which gives a reactor length-diameter ratio of about 0.8 and a fuel-element-passage L/d of over 400. Figure 7 shows that the optimum T_e is slightly greater than 5230° R, only about 200° below $T_{fe,max}$.

All curves in figures 5 to 7 are very flat, in the sense that illustrated variations in W_{RL} are small in relation to the magnitude of the residual load. Consequently, the optimum values of the various parameters are not well defined, and large deviations from the optimum point could be tolerated. For example, figure 5(d) shows that A_{ff} could be reduced from 6 to 4 square feet with less than 1 percent reduction in W_{RL}. The corresponding pressure (fig. 5(c)) would be about 600 instead of 400 pounds per square inch absolute. Similarly, P_e (fig. 6(d)) could be reduced by a factor of 2 (to 200 instead of 400 lb/sq in. abs) with almost no loss in W_{RL} provided that the flow area (fig. 6(c)) was about 7.5 square feet. Figures 5(d) and 6(d) also show that a reduction in L_R from 4 to 3.5 feet would penalize the overall performance by less than 1 percent of maximum W_{RL}.

Optimization of Initial Thrust-Weight Ratio

Previous studies (e.g., refs. 1, 2, and 12) have indicated that optimum initial thrust-weight ratio F/W_G for orbital launch of nuclear rockets is about 0.2 to 0.4. The data presented in figure 8 substantiate the earlier conclusions; maximum W_{RL} for all P_e corresponds to F/W_G slightly under 0.3. Reactor length does not appear to affect the optimization significantly. Only the highest portions of the envelope curves are drawn in figure 8 because the high-thrust cases required to extend the envelopes would have necessitated values of A_{ff} beyond the available reactor data.

At a thrust-weight ratio of 0.28, the thrust is 280,000 pounds and the reactor power is approximately 6600 megawatts. The corresponding reactor-power density, computed by dividing the total power by the total reactor volume, is about 80 megawatts per cubic foot. In the core of a reflected reactor, the optimum power density would be about 25 percent higher.

The existence of an optimum power density means that pushing the power density of a given reactor design to the limit is undesirable. For a given core type and general configuration, the optimum flow area, pressure, and length will generally result in a power density far below the maximum attainable value. This is equivalent to stating that as long as specific impulse is related to pressure and reactor dimensions,

as in the case analyzed herein, maximum powerplant thrust-weight ratio (or minimum powerplant specific weight) is not the best basis for design selection.

Because of the expanded W_{RL} scale, the illustrated variations due to changes in F/W_G are very small. All computed values of W_{RL} fall within a 10 percent spread. Thus, without sacrificing more than 3 or 4 percent of maximum residual load, the thrust-weight ratio and the reactor-power density could be cut in half. This decrease in power density would probably be accomplished by operating at values of reactor-exit pressure and dynamic pressure about one-half of the optimum values (i.e., about 200 and 10 lb/sq in., respectively). The estimated penalty of 3 or 4 percent is based on unpublished calculations since only one value of q_e was used in the study reported herein.

Effect of Assumptions

Since the optimization of powerplant parameters is chiefly the achievement of a balance between opposing trends in propellant and powerplant weights, any assumptions that affect these weights significantly will affect the results of the optimization. For example, the assumption that turbine exhaust contributes no propulsive thrust magnifies the penalty in specific impulse due to bleed flow. A more comprehensive analysis should involve the determination of bleed-flow specific impulse and of the fraction of control-jet thrust, that contributes to vehicle propulsion. Another such assumption is that of equilibrium expansion in the nozzle; this assumption favors low pressures because of the increase in I_{vac} resulting from recombination. If the nozzle gas state were somewhere between equilibrium and frozen, optimum pressure would be somewhat higher than the values indicated herein.

Among the various components of the powerplant, only two are of sufficient magnitude to have much effect on the overall optimization. Reactor weight is one component; the selection of a water-moderated reactor produces a lower optimum reactor power than would have been obtained for a system employing a reactor of more nearly constant weight. Optimum flow area is also higher because of this moderator choice. The other prominent component weight is (or could be) that of the nuclear shield. In this study, a relatively lightweight shield, which is intended only to prevent excessive boiloff in the propellant tank is included. Should the reference shield weight be considerably higher, in order to provide biological shielding or to protect a more closely coupled tank, the optimization would be more sensitive to changes in flow area. As a result, optimum A_{ff} would be lower and optimum P_e would be higher.

Specified values of gross weight and hyperbolic velocity will influence the optimization to the extent that they affect the relative magnitudes of propellant and powerplant weights. As vehicle weight is increased, the powerplant becomes smaller in proportion to the propellant weight, and residual load will be less sensitive to changes in powerplant parameters. On the other hand, as hyperbolic velocity increases, the propellant will constitute an increasingly greater part of the total vehicle weight. As a result, those factors that influence I_{eff} and F/W_G will become more significant as the mission becomes more difficult.

The assumed value of minimum fuel-element spacing has a strong effect on the optimization of reactor length. Optimum fuel-element length-diameter ratio tends to remain relatively fixed for a particular type of system. Consequently, optimum L_R will tend to vary directly with s_{fe}. Other limit variables, such as dynamic pressure and fuel-element temperature, will probably have only a small influence on the overall optimization. The assumed value of q_e will enter into the relation between P_e and G_R and, thereby, affect the fuel-element heat transfer. The increase in optimum P_e corresponding to reduction in q_e from 20 to 10 pounds per square inch, however, is not expected to be more than 20 percent.

CONCLUDING REMARKS

The twofold purpose of this report is to (1) present a method of powerplant parameter optimization, and (2) illustrate the technique with a sample calculation. Accordingly, the assumptions and equations have been listed in detail. The example gives a qualitative insight into the interactions of the various powerplant and vehicle characteristics. Although the calculations have been carried out for a particular set of assumptions and specifications, the resulting trends and relations are instructive in a more general sense.

The specific results apply to nuclear rockets that employ advanced reactors, typified by the water-moderated, tungsten 184 fuel-element concept used herein, and that have initial weights in orbit of about 1,000,000 pounds. This gross weight and the specified velocity requirement of the mission are typical of the earth-escape portion of a manned vehicle for Mars exploration. Thus the situation that has been analyzed is the application of an advanced nuclear-rocket powerplant to a manned interplanetary mission starting from Earth orbit.

The results show that the attainment of high specific impulse is a strong factor in the optimization of such powerplant parameters as

reactor flow area, reactor-exit pressure, and reactor length. The importance of achieving low reactor-exit pressure, high reactor-exit temperature, and low bleed flow rate is shown to be great enough to make optimum pressure only about 400 pounds per square inch absolute. The corresponding reactor flow area is approximately 6 square feet, which gives an optimum reactor power density of only about 80 megawatts per cubic foot. Thus, the attainment of high specific impulse is of more importance than the attainment of minimum powerplant specific weight.

Residual load is not very sensitive to changes in the optimization parameters, especially at large values of vehicle gross weight. Consequently, large deviations from the optimum values of reactor flow area, reactor-exit total pressure, and reactor length correspond to losses in residual load of only 1 or 2 percent. Initial thrust-weight ratio can probably be reduced by a factor of 2 from the optimum value of about 0.3 with a loss in residual load of only 3 to 4 percent of the residual load. Reactor-power density can be reduced proportionately if the thrust is lowered by making changes in dynamic pressure and reactor-exit total pressure rather than in reactor dimensions.

The optimization technique described herein can be used to evaluate many of the complex interrelations among powerplant components. With slight modifications it can be used to study other types of nuclear-rocket powerplants. In this way the areas of most sensitivity can be revealed early in the nuclear-rocket research and development process, and primary attention can be directed toward those areas where the largest gains are possible.

Lewis Research Center
National Aeronautics and Space Administration
Cleveland, Ohio, August 1, 1962

APPENDIX - SYMBOLS

A	cross-sectional area
b	thickness
c_p	specific heat at constant pressure
D	diameter
d	hydraulic diameter
F	thrust
f	Fanning friction factor
G	mass velocity, w/A
g	weight-to-mass conversion factor, 32.174 lb/slug
h	heat-transfer coefficient
I_{eff}	effective specific impulse
I_{vac}	specific impulse in vacuum
k	thermal conductivity
k_{eff}	effective multiplication factor
L	length
M	Mach number
N	number
Nu	Nusselt number
P	total pressure
Pr	Prandtl number
p	static pressure
Q	power
q	heat flux

q_e dynamic pressure at reactor exit

R gas constant for hydrogen

Re Reynolds number

S surface area

s spacing

T total temperature

t static temperature

V velocity

W weight

w weight flow rate

x axial distance

γ ratio of specific heats

η effectiveness

θ temperature difference between hot and cold streams

ρ weight density

σ design stress

Subscripts:

aw adiabatic wall

BP booster pump

b bulk

C convergent section

c coolant side

e reactor exit

F fin

f film

fe	fuel element
ff	free flow
G	gross (initial)
g	hot gas side
h	hyperbolic
i	reactor-core inlet
in	inner, heat-exchanger tube
m	moderator
max	maximum
N	nozzle
N,e	nozzle coolant-side exit
N,i	nozzle coolant-side inlet
NS	nuclear shield
out	outer, heat-exchanger tube
P	propellant
PC	powerplant control system
PS	pressure shell
R	reactor
RC	reactor control system
RL	residual load
ref	reference design
SP	start system and piping
ST	vehicle structure
T	tank

TP	turbopump
TP, e	turbopump exit
t	tubes
v	void
W	tungsten
WP	water pump
w	wall
X	heat exchanger
X, e	heat-exchanger exit
X, i	heat-exchanger inlet
β	bleed
1	cold end
2	hot end

Superscript:

*	nozzle throat

E-1479

REFERENCES

1. Johnson, Paul G., and Smith, Roger L.: An Optimization of Powerplant Parameters for Orbital-Launch Nuclear Rockets. NASA TN D-675, 1961.

2. Cavicchi, Richard H., and Miser, James W.: Determination of Nuclear-Rocket Power Levels for Unmanned Mars Vehicles Starting from Orbit About Earth. NASA TN D-474, 1962.

3. Ellerbrock, Herman H., Cavicchi, Richard H., Duscha, Rudolph A., and Linke, Heinz G.: Systems Design of Unmanned Nuclear-Powered Mars Vehicles Starting from Orbit About Earth. NASA TM X-486, 1962.

4. Einstein, Thomas H.: Analysis of Heat Transfer and Pressure Drop for a Gas Flowing Between a Set of Multiple Parallel Flat Plates at High Temperatures. NASA TN D-1165, 1961.

5. Hyland, Robert E.: Reactor Weight Study Using Beryllium Oxide, Beryllium, Lithium Hydride, and Water as Moderators with Tungsten 184 Structural Material and Uranium Dioxide Fuel. NASA TN D-1407, 1962.

6. Thornton, Gunnar, and Blumberg, Ben: ANP HTREs Fulfill Test Goals. Nucleonics, vol. 19, no. 1, Jan. 1961, pp. 45-51.

7. King, Charles R.: Compilation of Thermodynamic Properties, Transport Properties, and Theoretical Rocket Performance of Gaseous Hydrogen. NASA TN D-275, 1960.

8. Hilsenrath, Joseph, et al.: Tables of Thermal Properties of Gases. Cir. 564, NBS, Nov. 1, 1955.

9. Hendricks, R. C., Graham, R. W., Hsu, Y. Y., and Medeiros, A. A.: Correlation of Hydrogen Heat Transfer in Boiling and Supercritical Pressure States. ARS Jour., vol. 32, no. 2, Feb. 1962, pp. 244-251.

10. Ginsburg, A. A., Stewart, W. L., and Hartmann, M. J.: Turbopumps for High-Energy Propellants. Paper 59-53, Inst. Aero. Sci., Inc., 1959.

11. Moeckel, W. E.: Trajectories with Constant Tangential Thrust in Central Gravitational Fields. NASA TR R-53, 1960.

12. Himmel, S. C., Dugan, J. F., Jr., Luidens, R. W., and Weber, R. J.: A Study of Manned Nuclear-Rocket Missions to Mars. Paper 61-49, Inst. Aero. Sci., Inc., 1961.

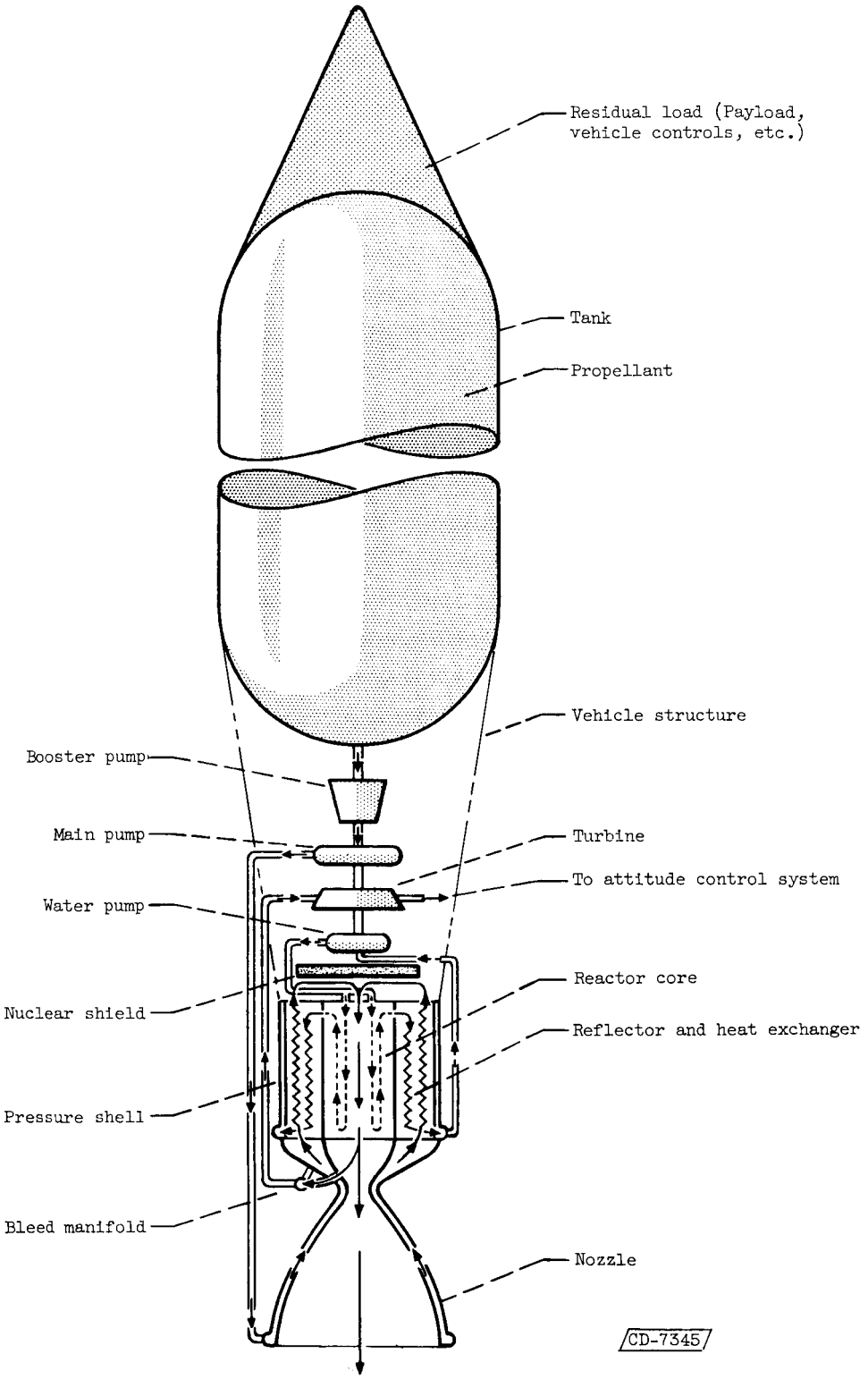

Figure 1. - Schematic diagram of nuclear rocket showing propellant and moderator flow circuits.

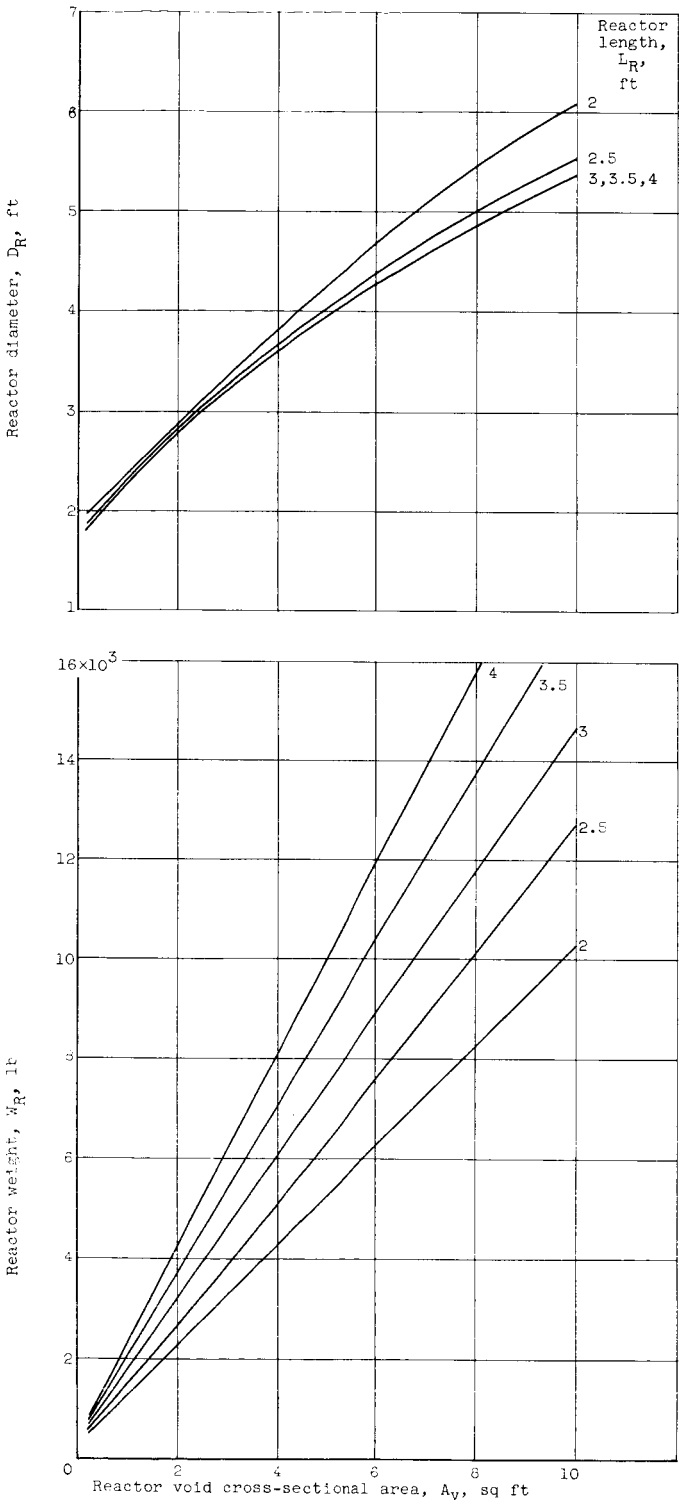

Figure 2. - Variation of reactor diameter and weight with void area and reactor length. Effective multiplication factor, 1.05; moderator, water; fuel-containing material, tungsten 184 (78 volume percent); volume ratio of uranium dioxide to uranium dioxide plus tungsten, 0.15; weight of tungsten per unit of void volume, 400 pounds per cubic foot; uranium 235 enrichment, 93 percent.

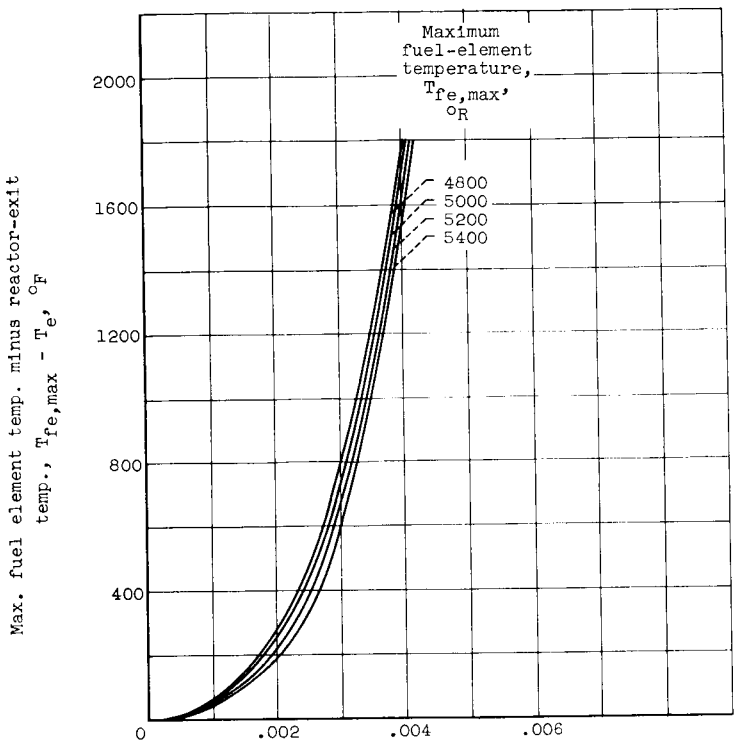

(a) Variation of difference between maximum fuel-element temperature and reactor-exit temperature with flow-geometry parameter and maximum fuel-element temperature.

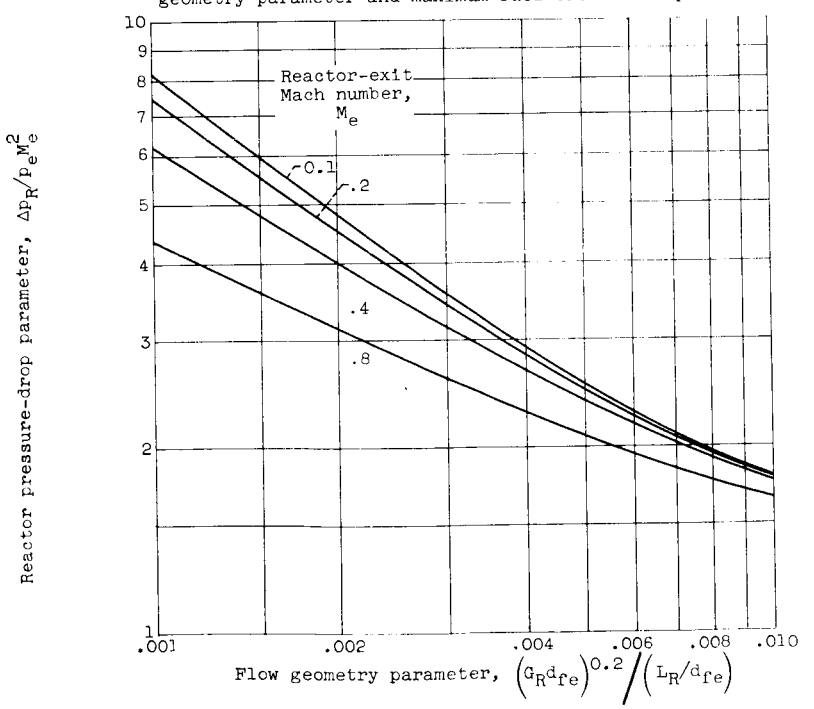

(b) Variation of reactor pressure-drop parameter with flow-geometry parameter and reactor-exit Mach number.

Figure 3. - Reactor heat-transfer and pressure-drop characteristics.

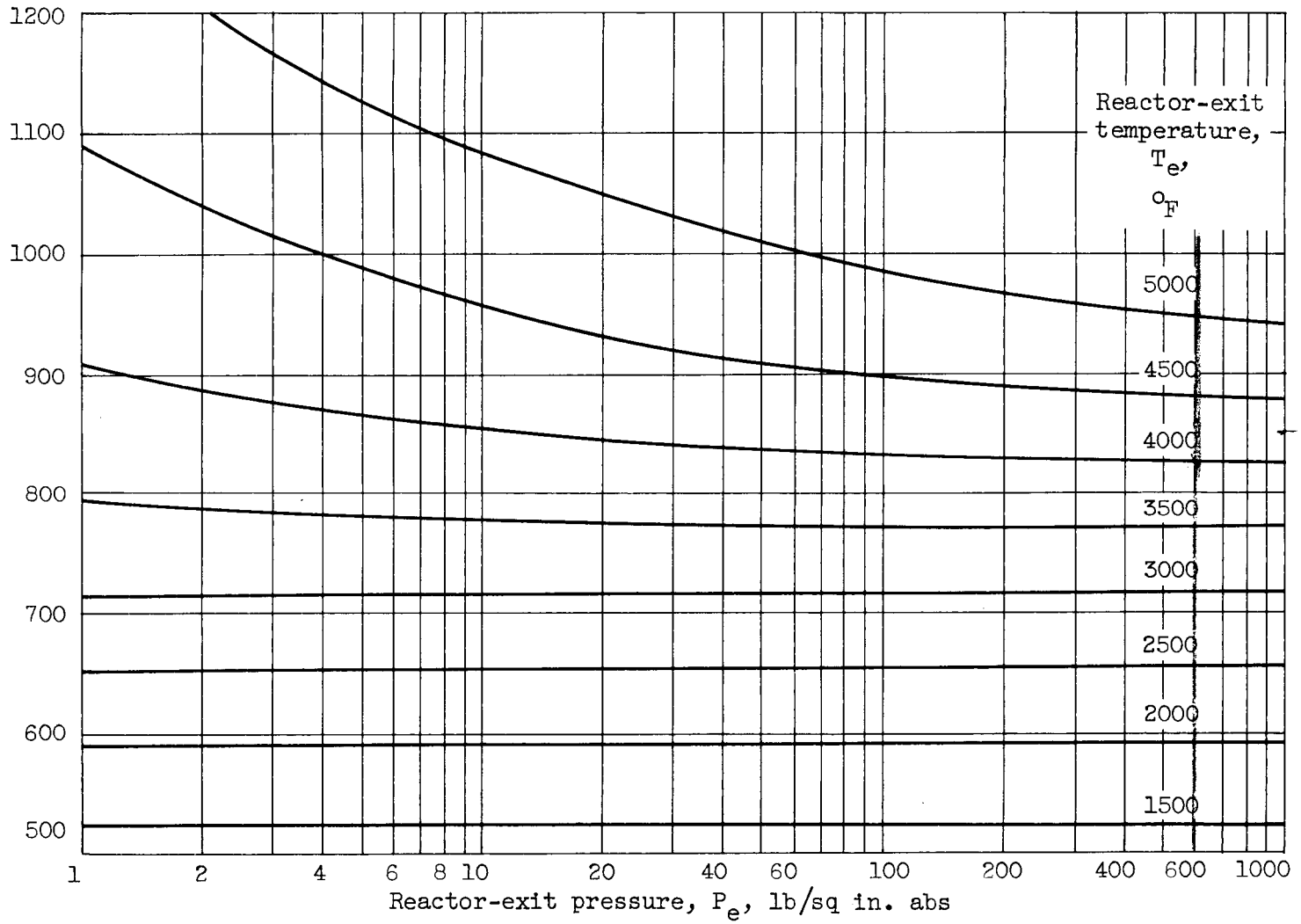

Figure 4. - Variation of specific impulse in vacuum with reactor-exit hydrogen conditions. Nozzle area ratio, 50; equilibrium expansion; velocity correction factor, 0.96.

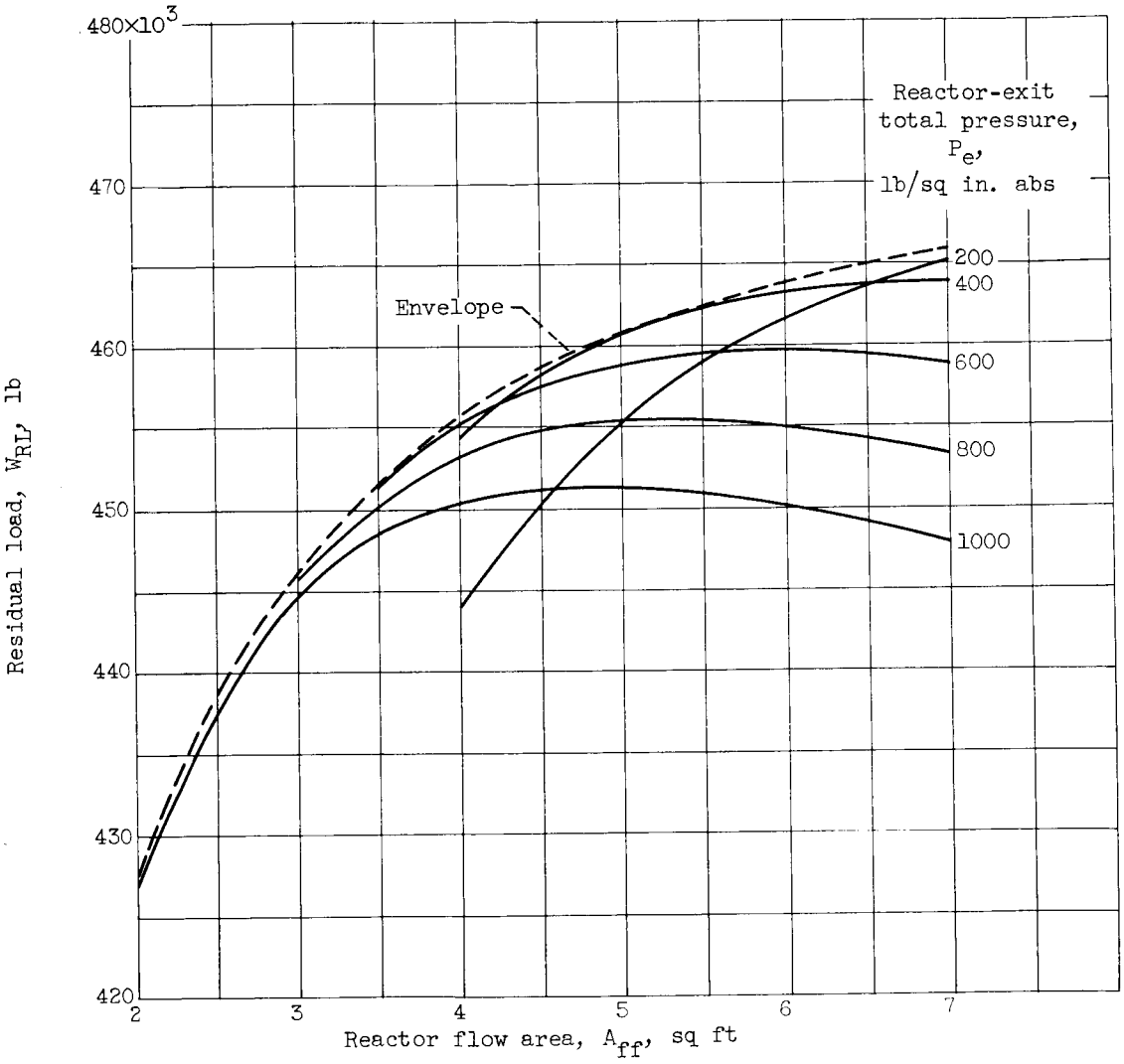

(a) Effect of reactor-exit total pressure. Reactor length, 3 feet.

Figure 5. - Variation of residual load with reactor flow area.

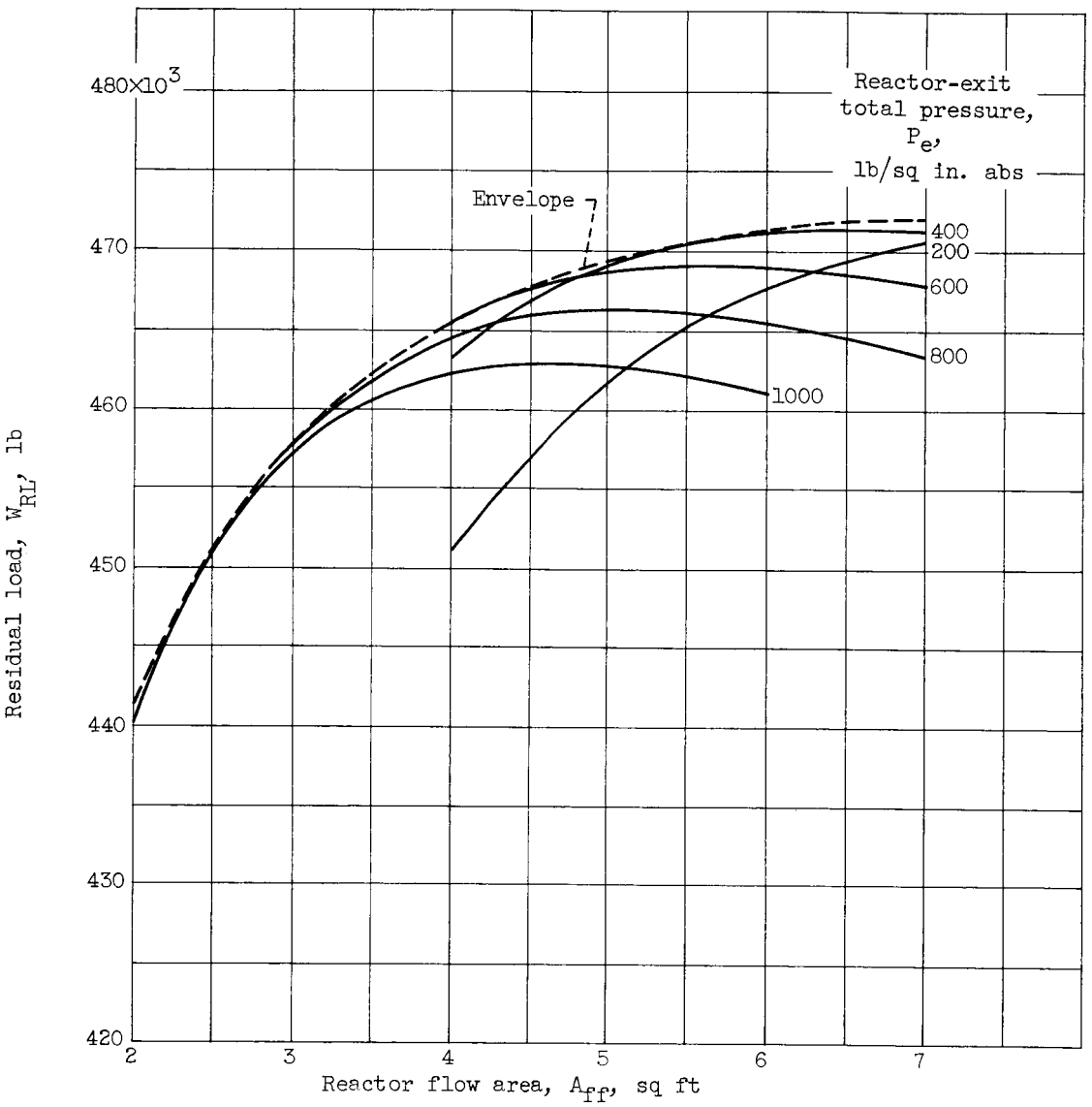

(b) Effect of reactor-exit total pressure. Reactor length, 3.5 feet.

Figure 5. - Continued. Variation of residual load with reactor flow area.

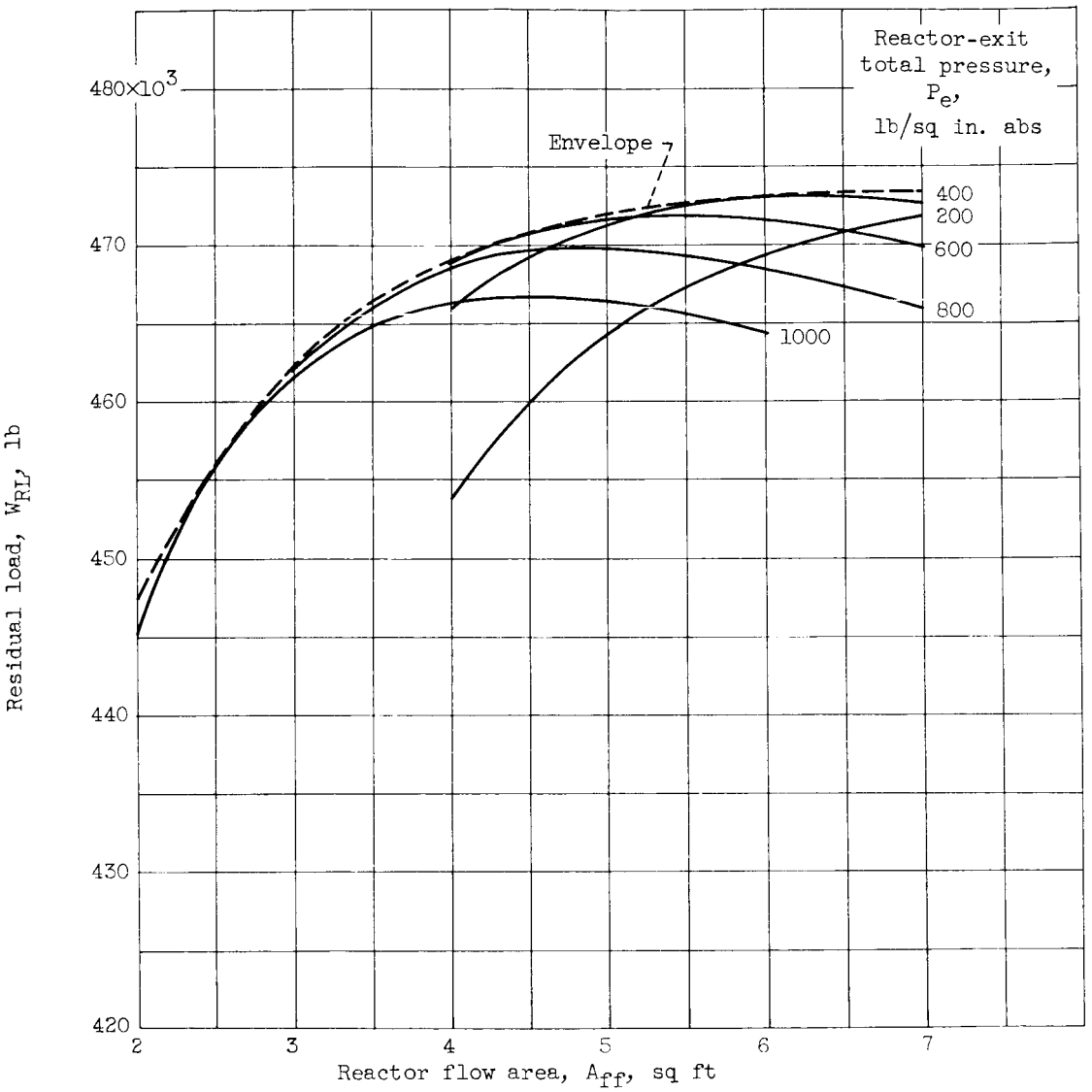

(c) Effect of reactor-exit total pressure. Reactor length, 4 feet.

Figure 5. - Continued. Variation of residual load with reactor flow area.

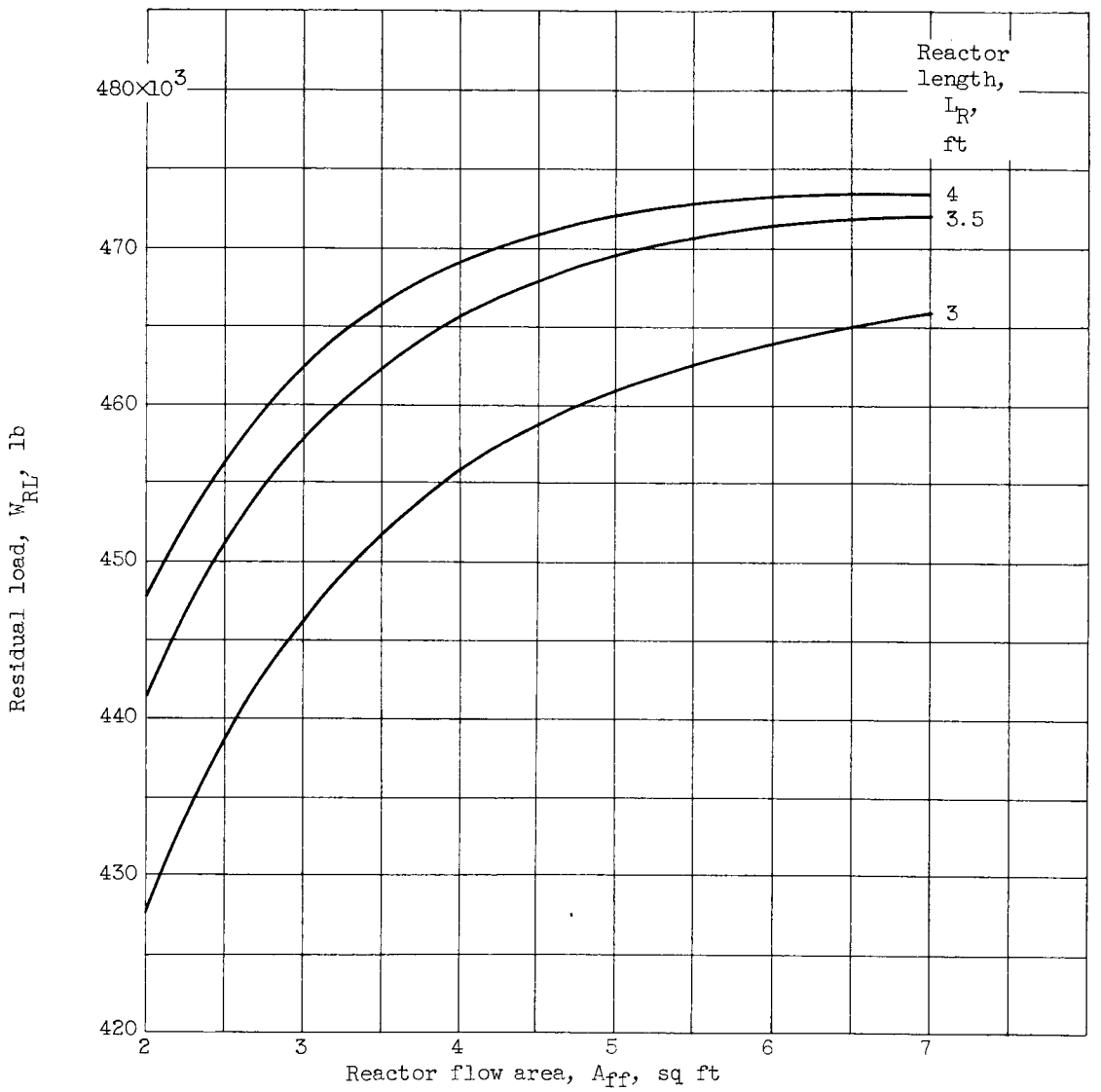

(d) Comparison of envelope curves.

Figure 5. - Concluded. Variation of residual load with reactor flow area.

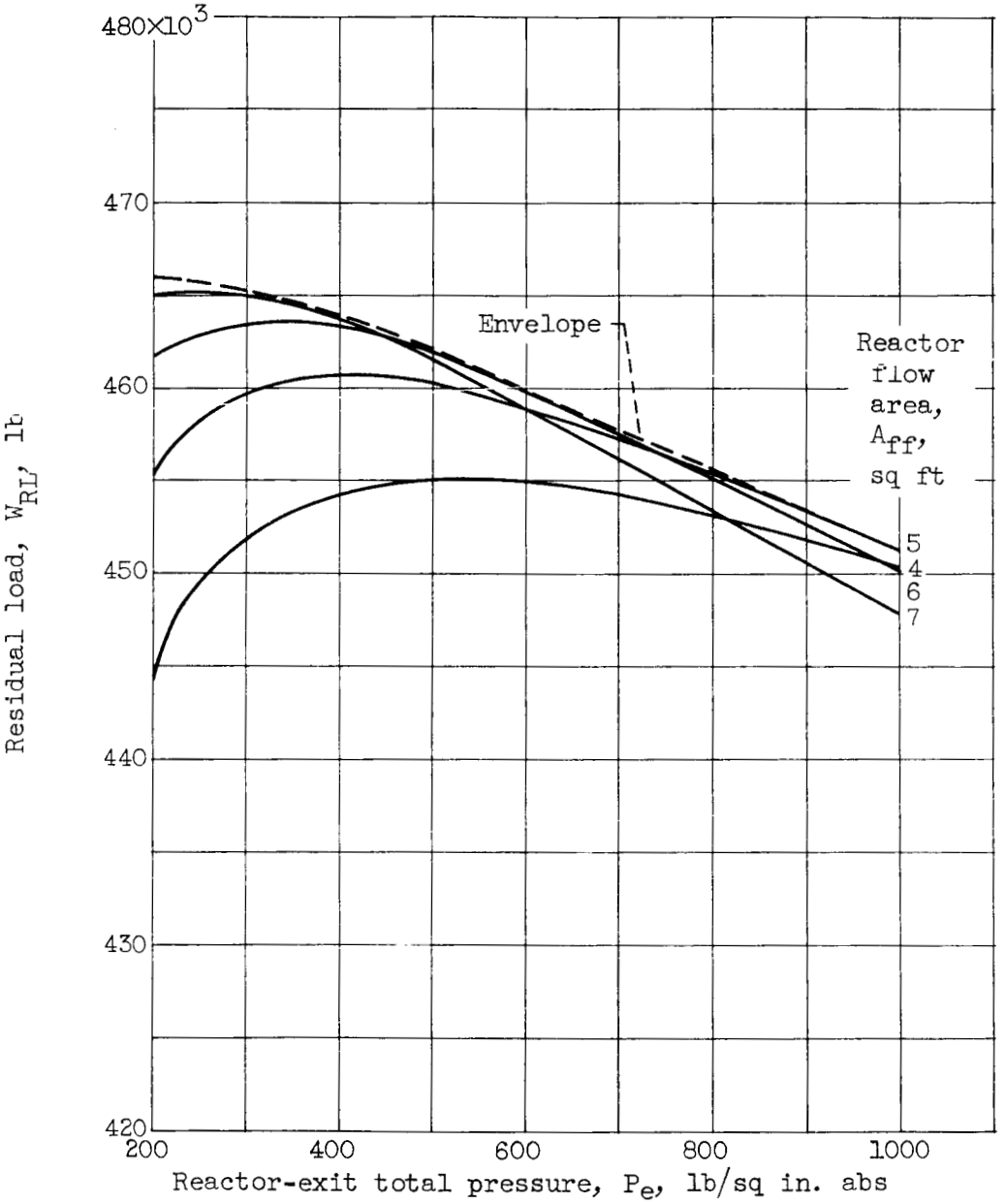

(a) Effect of reactor flow area. Reactor length, 3 feet.

Figure 6. - Variation of residual load with reactor-exit total pressure.

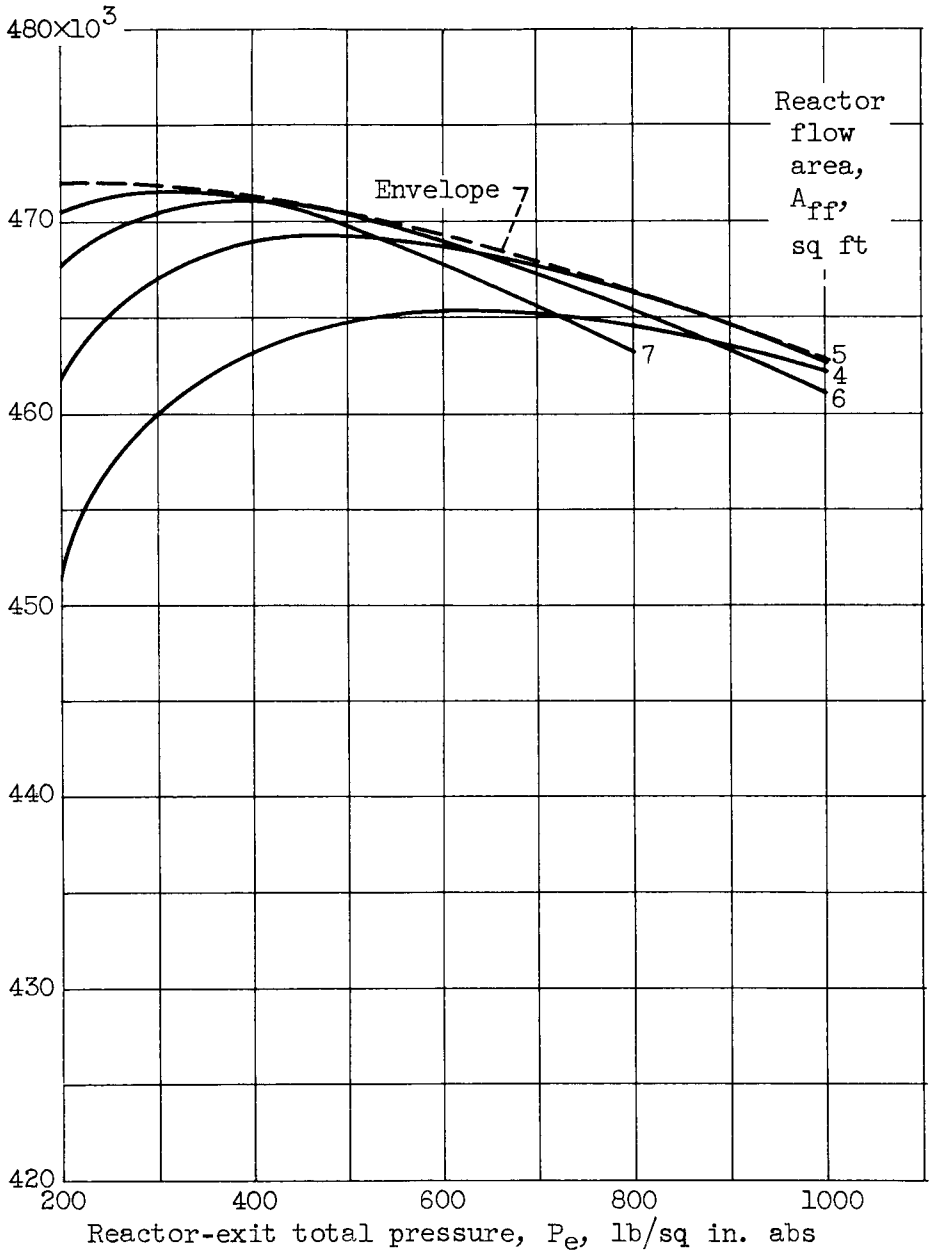

(b) Effect of reactor flow area. Reactor length, 3.5 feet.

Figure 6. - Continued. Variation of residual load with reactor-exit total pressure.

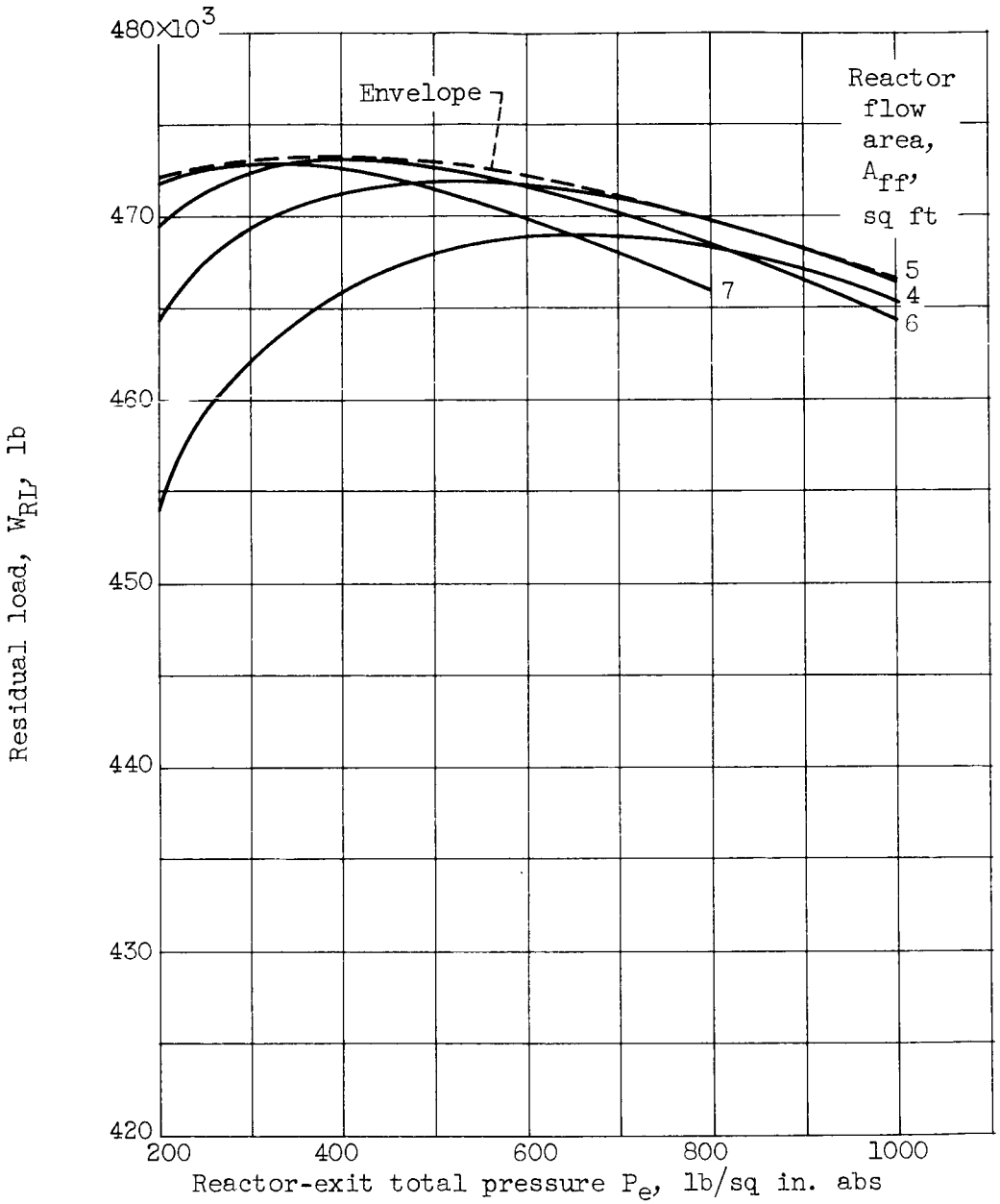

(c) Effect of reactor flow area. Reactor length, 4 feet.

Figure 6. - Continued. Variation of residual load with reactor-exit total pressure.

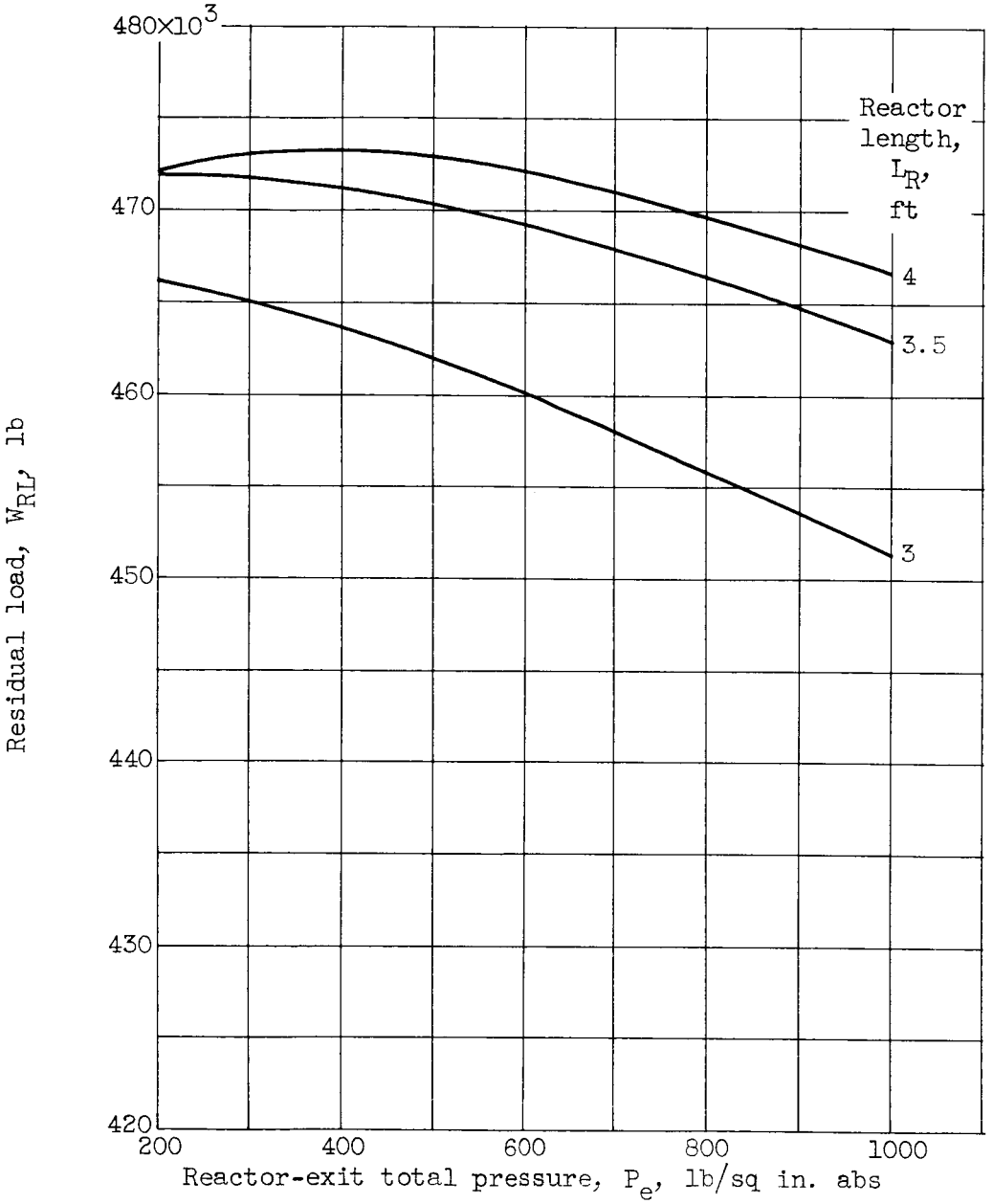

(d) Comparison of envelope curves.

Figure 6. - Concluded. Variation of residual load with reactor-exit total pressure.

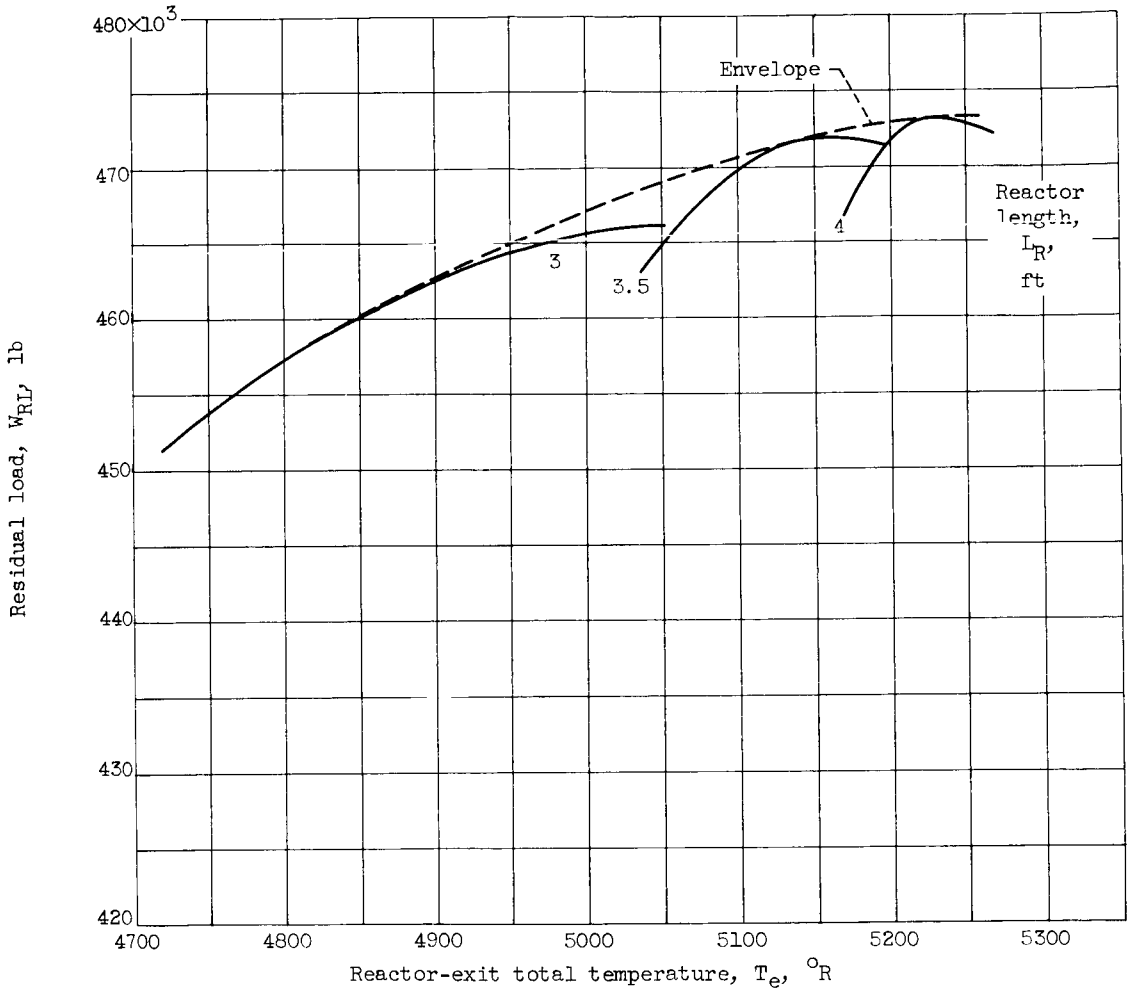

Figure 7. - Variation of residual load with reactor-exit total temperature for various reactor lengths.

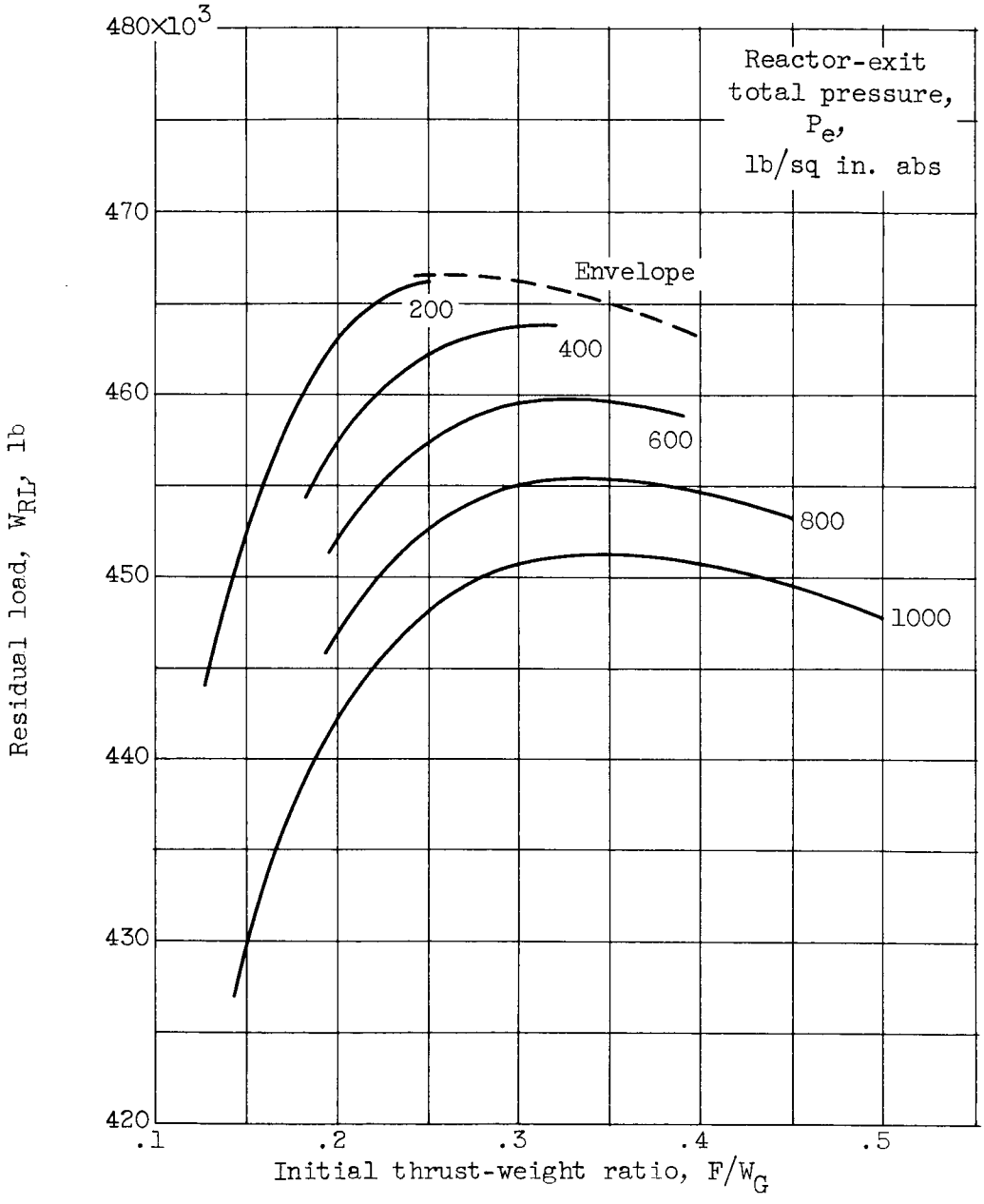

(a) Reactor length, 3 feet.

Figure 8. - Effect of reactor-exit total pressure on variation of residual load with initial thrust-weight ratio.

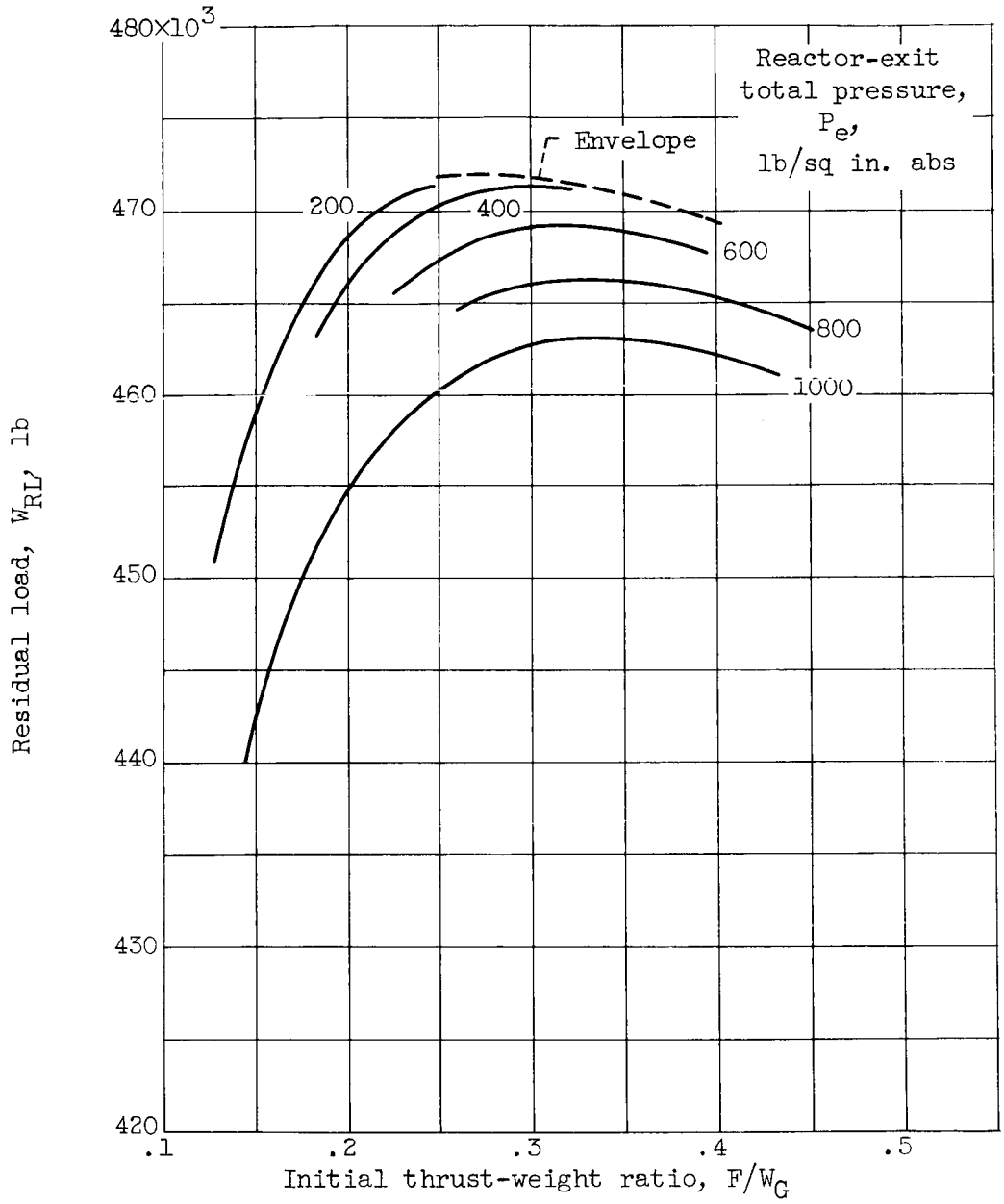

(b) Reactor length, 3.5 feet.

Figure 8. - Continued. Effect of reactor-exit total pressure on variation of residual load with initial thrust-weight ratio.

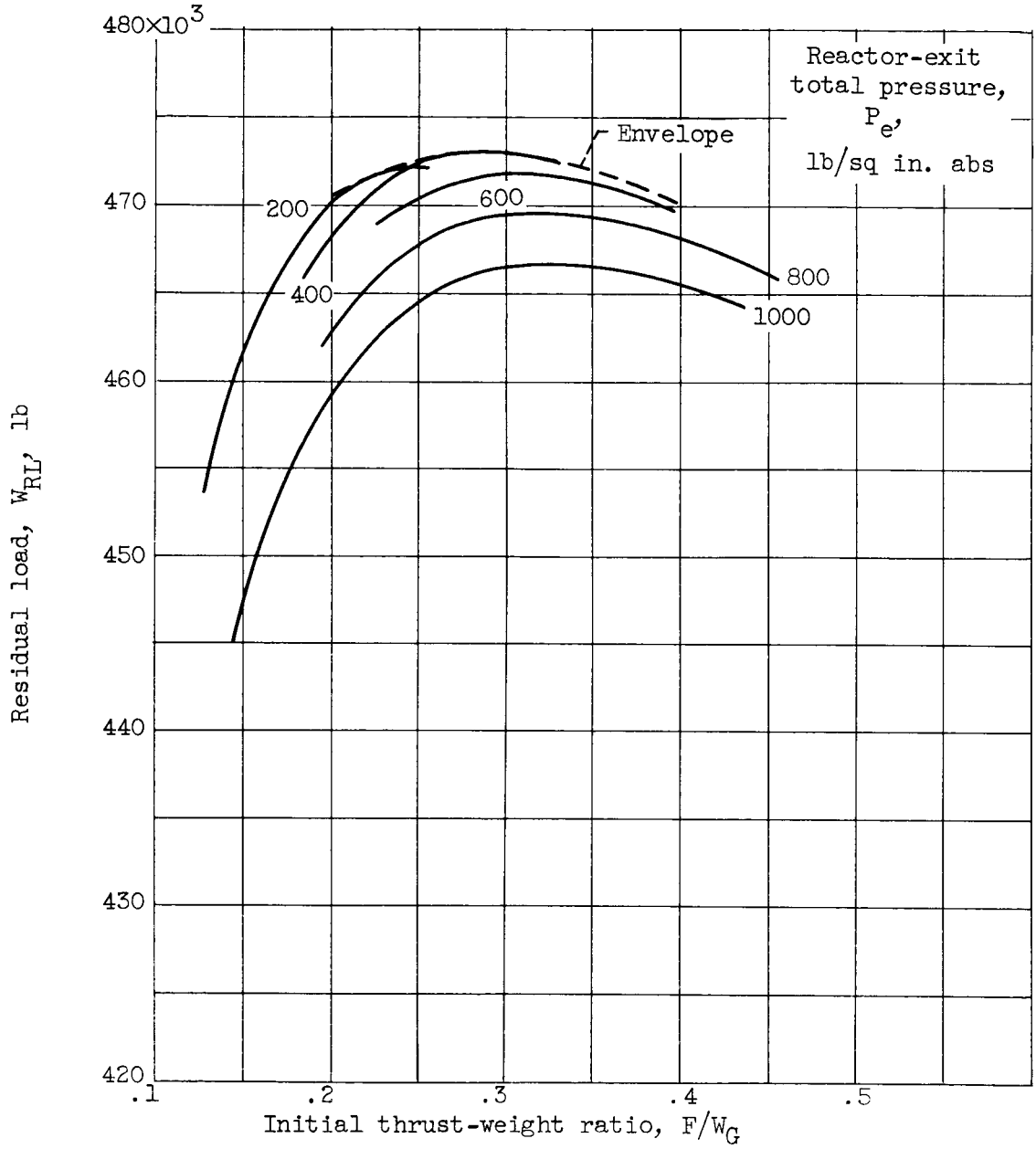

(c) Reactor length, 4 feet.

Figure 8. - Concluded. Effect of reactor-exit total pressure on variation of residual load with initial thrust-weight ratio.

NASA TM X-717
National Aeronautics and Space Administration
OPTIMIZATION OF NUCLEAR-ROCKET POWER-PLANT PARAMETERS. Paul G. Johnson, Glenn R. Cowgill, and James W. Miser. February 1963.
47 p., diags.
(NASA TECHNICAL MEMORANDUM X-717)

The method presented in detail is illustrated with an example corresponding to the initial phase of a manned Mars exploration mission. The analysis determines values of reactor flow area, reactor-exit pressure, and reactor length that produce maximum residual load. The optimization is shown to be relatively insensitive to off-optimum changes in these powerplant parameters. The attainment of high specific impulse is shown to be more important than the attainment of maximum reactor-power density or minimum powerplant specific weight.

Copies obtainable from NASA, Washington

[redacted]

I. Johnson, Paul G.
II. Cowgill, Glenn R.
III. Miser, James W.
IV. NASA TM X-717

(Initial NASA distribution: 42, Propulsion systems, nuclear.)

NASA

[redacted]

NASA TM X-717
National Aeronautics and Space Administration
OPTIMIZATION OF NUCLEAR-ROCKET POWER-PLANT PARAMETERS. Paul G. Johnson, Glenn R. Cowgill, and James W. Miser. February 1963.
47 p., diags.
(NASA TECHNICAL MEMORANDUM X-717)

The method presented in detail is illustrated with an example corresponding to the initial phase of a manned Mars exploration mission. The analysis determines values of reactor flow area, reactor-exit pressure, and reactor length that produce maximum residual load. The optimization is shown to be relatively insensitive to off-optimum changes in these powerplant parameters. The attainment of high specific impulse is shown to be more important than the attainment of maximum reactor-power density or minimum powerplant specific weight.

Copies obtainable from NASA, Washington

[redacted]

I. Johnson, Paul G.
II. Cowgill, Glenn R.
III. Miser, James W.
IV. NASA TM X-717

(Initial NASA distribution: 42, Propulsion systems, nuclear.)

NASA

[redacted]

NASA TM X-717
National Aeronautics and Space Administration
OPTIMIZATION OF NUCLEAR-ROCKET POWER-PLANT PARAMETERS. Paul G. Johnson, Glenn R. Cowgill, and James W. Miser. February 1963.
47 p., diags.
(NASA TECHNICAL MEMORANDUM X-717)

The method presented in detail is illustrated with an example corresponding to the initial phase of a manned Mars exploration mission. The analysis determines values of reactor flow area, reactor-exit pressure, and reactor length that produce maximum residual load. The optimization is shown to be relatively insensitive to off-optimum changes in these powerplant parameters. The attainment of high specific impulse is shown to be more important than the attainment of maximum reactor-power density or minimum powerplant specific weight.

Copies obtainable from NASA, Washington

[redacted]

I. Johnson, Paul G.
II. Cowgill, Glenn R.
III. Miser, James W.
IV. NASA TM X-717

(Initial NASA distribution: 42, Propulsion systems, nuclear.)

[redacted]

NASA TM X-717
National Aeronautics and Space Administration
OPTIMIZATION OF NUCLEAR-ROCKET POWER-PLANT PARAMETERS. Paul G. Johnson, Glenn R. Cowgill, and James W. Miser. February 1963.
47 p., diags.
(NASA TECHNICAL MEMORANDUM X-717)

The method presented in detail is illustrated with an example corresponding to the initial phase of a manned Mars exploration mission. The analysis determines values of reactor flow area, reactor-exit pressure, and reactor length that produce maximum residual load. The optimization is shown to be relatively insensitive to off-optimum changes in these powerplant parameters. The attainment of high specific impulse is shown to be more important than the attainment of maximum reactor-power density or minimum powerplant specific weight.

Copies obtainable from NASA, Washington

[redacted]

I. Johnson, Paul G.
II. Cowgill, Glenn R.
III. Miser, James W.
IV. NASA TM X-717

(Initial NASA distribution: 42, Propulsion systems, nuclear.)

[redacted]